Structure−Reactivity Relationships in Rare-Earth Metal Carboxylate-Based Binary Ziegler-Type Catalysts

Andreas Fischbach,† Franc Perdih,† Eberhardt Herdtweck,† and Reiner Anwander*,‡

Department Chemie, Lehrstuhl Für Anorganische Chemie, Technische Universität München, Lichtenbergstrasse 4, D-85747 Garching, Germany, and Department of Chemistry, University of Bergen, Allégaten 41, N-5007, Bergen, Norway

Received January 18, 2006

The organoaluminum-mediated alkylation of tailor-made rare-earth metal carboxylate complexes was studied, and implications of the degree of Ln alkylation and organoaluminum-chloride-mediated cation formation for 1,3-diene polymerization were investigated. Highly substituted rare-earth metal benzoate complexes $\{Ln(O_2CC_6H_2Me_3\text{-}2,4,6)_3\}_n$ (Ln = Y, La, Nd), $\{Ln(O_2CC_6H_2iPr_3\text{-}2,4,6)_3\}_n$ (Ln = Y, La, Nd, Gd, Lu), $\{Ln(O_2CC_6H_2tBu_3\text{-}2,4,6)_3(THF)\}_n$ (Ln = Y, La), $\{Ln(O_2CC_6H_3Ph_2\text{-}2,6)_3(THF)\}_n$ (Ln = Y, La), and $\{Ln(O_2CC_6H_3Mes_2\text{-}2,6)_3(THF)\}_n$ (Ln = Y, La) were obtained quantitatively according to the silylamide route from $Ln[N(SiMe_3)_2]_3$ and alkyl(aryl)-substituted benzoic acids. Such oligomeric carboxylate complexes are insoluble in aliphatic and aromatic solvents, but could be crystallized from donor solvents such as THF, DMSO, and pyridine. X-ray crystallographic analyses indicated the formation of monomeric $[Nd(O_2CC_6H_2Me_3\text{-}2,4,6)_3(DMSO)_3]$ and dimeric $[La(O_2CC_6H_2Me_3\text{-}2,4,6)_2(\mu\text{-}O_2CC_6H_2Me_3\text{-}2,4,6)\text{-}(DMSO)_2]_2$ depending on the metal ion size. Depending on the steric demand of the benzoate ligands, mono- and bis(tetraalkylaluminate) complexes $[Me_2Al(O_2CC_6H_2iPr_3\text{-}2,4,6)_2]_2Ln[(\mu\text{-}Me)_2AlMe_2]$ and $\{Ln(O_2CC_6H_2tBu_3\text{-}2,4,6)[(\mu\text{-}Me)_2AlMe_2]_2\}_2$, respectively, could be identified as major product components from the reaction with excess AlR_3 (R = Me, Et), by means of ^1H NMR spectroscopy and X-ray structure analysis. When activated with Et_2AlCl, the resulting binary Ziegler-type catalysts efficiently polymerized isoprene (>99% *cis*-1,4), the polymerization performance depending on the metal center (Nd > Gd > La) and the degree of alkylation ("$Ln(AlMe_4)_2$" > "$Ln(AlMe_4)$"). Equimolar reaction of $[Me_2Al(O_2CC_6H_2iPr_3\text{-}2,4,6)_2]_2Ln[(\mu\text{-}Me)_2AlMe_2]$ with R_2AlCl (R = Me, Et) quantitatively produced $[Me_2Al(O_2CC_6H_2iPr_3\text{-}2,4,6)]_2$, proposing "$Me_2LnCl$" as the polymerization-initiating species. Homoleptic $Ln(AlMe_4)_3$ was spotted as a crucial reaction intermediate and was used for the high-yield synthesis of the various alkylated carboxylate complexes according to a novel "tetraalkylaluminate" route.

Introduction

Multicomponent Ziegler−Natta catalysts implicating 3d and 4f transition metal inorganics and organoaluminum compounds display efficient polymerization initiators for the industrial manufacture of polyolefins such as polypropylene, polybutadiene, and polystyrene.[1] Although these "first-generation" catalysts are often superior to more sophisticated metallocene and postmetallocene congeners, details of the polymerization mechanisms and the formation of catalytically active centers have remained scarce, and hence improvement and optimization of the catalytic system have been achieved only empirically.[1] Cationic metal alkyl or hydrido sites are often proposed to display the active species promoting monomer insertion and chain elongation.[1] In organolanthanide catalysis, Ziegler−Natta-type multicomponent systems represent the only class of homogeneous catalysts of considerable commercial relevance.[2−6] High *cis*-1,4-polydienes are industrially produced from 1,3-dienes (butadiene and isoprene) in aliphatic or aromatic hydrocarbons by a number of Ziegler−Natta-type catalysts based on the transition metals titanium, cobalt, and nickel and the lanthanide element neodymium.[2−9] The formation of polymers with the highest *cis*-1,4 contents (>98%) makes neodymium-based butadiene rubbers superior with respect to abrasion and cracking resistance, tack (the ability of the polymer to stick to itself), and raw polymer strength.[10,11] Therefore, these polymers are particularly useful for the production of high-performance tires. Numerous binary and ternary neodymium catalytic systems have been designed empirically and investigated since the early discoveries in the 1960s. Commonly used neodymium-based

* To whom correspondence should be addressed. Fax: +47 555 8949. E-mail: reiner.anwander@kj.uib.no.

† Technische Universität München.

‡ University of Bergen.

(1) (a) *Ziegler Catalysts*; Fink, G., Mühlhaupt, R., Brintzinger, H.-H., Eds.; Springer-Verlag: Berlin, 1995. (b) Mühlhaupt, R. *Macromol. Chem. Phys.* **2003**, *204*, 289. (c) Böhm, L. L. *Angew. Chem., Int. Ed.* **2003**, *42*, 5010.

(2) Shen, Z.; Ouyang, J. In *Handbook on the Physics and Chemistry of Rare Earths*; Gschneidner, K. A., Jr., Fleming, L., Eds.; Elsevier Science Publishers: The Netherlands, 1987; Chapter 61.

(3) Taube, R.; Sylvester, G. In *Applied Homogeneous Catalysis with Organometallic Compounds*; Cornils, B., Herrmann, W. A., Eds.; VCH: Weinheim, 2002; p 280.

(4) Thiele, K.-H.; Wilson, D. R. *J. Macromol. Sci., Polym. Rev.* **2003**, *C43*, 581.

(5) *Ullmann's Encyclopedia of Industrial Chemistry*, 5th ed.; VCH: Weinheim, 1993; Vol. A4, pp 221, 261.

(6) Porri, L.; Giarusso, A. In *Comprehensive Polymer Science*; Eastmond, G. C., Ledwith, A., Russo, S., Sigwalt, P., Eds.; Pergamon Press: Oxford, U.K., 1989; Vol. 4, Part II, p 53.

(7) Boor, J. *Ziegler−Natta Catalysts and Polymerizations*; Academic Press: New York, 1979; Vol. 17, p 130.

(8) Anwander, R. In *Applied Homogeneous Catalysis with Organometallic Compounds*; Cornils, B., Herrmann, W. A., Eds.; VCH: Weinheim, 2002; p 974.

(9) Yasuda, H. *Top. Organomet. Chem.* **1999**, *2*, 255.

(10) Wilson, D. J. *Makromol. Chem., Macromol. Symp.* **1993**, *66*, 273.

(11) Lauretti, E.; Miani, B.; Mistrali, F. *Rubber World* **1994**, *210*, 34.

10.1021/om060052i CCC: $33.50
Publication on Web 03/01/2006

Scheme 1. Proposed Activation Sequence of Oligomeric Ln(III) Carboxylates via Different Organoaluminum Cocatalysts According to the Literature;[15−20] Also Shown Are Commercially Employed "O_2XR" (X = C, P) Ligands

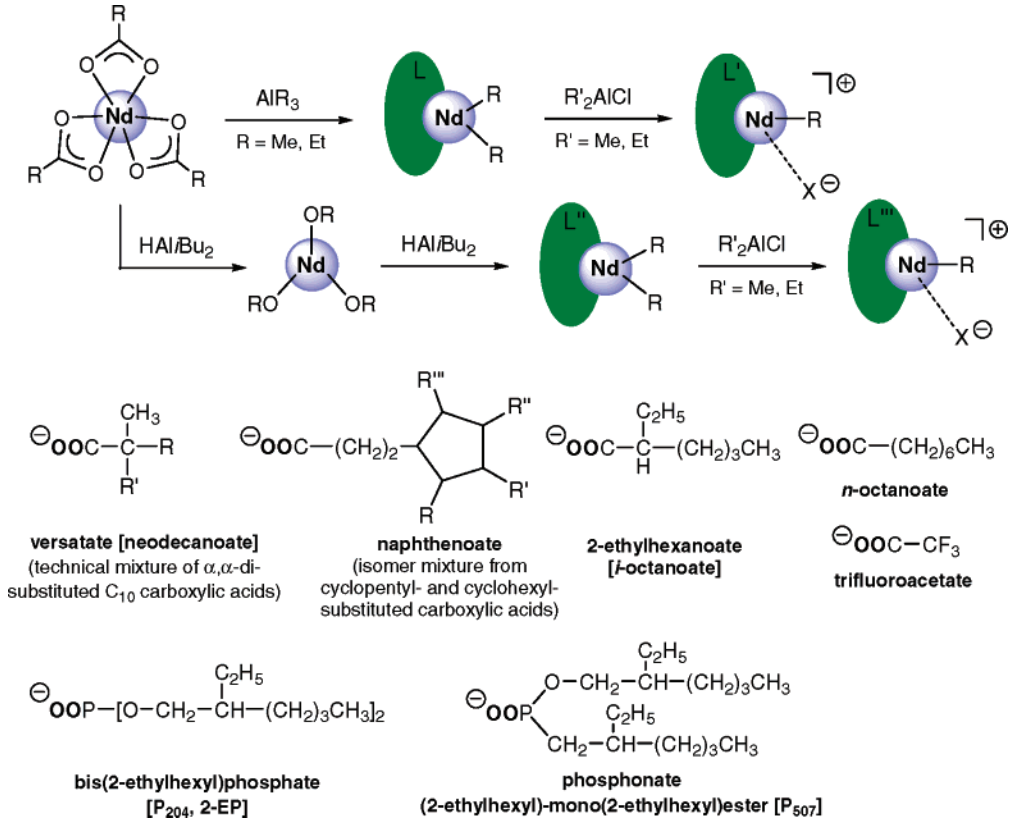

catalysts comprise Nd(III) carboxylates (also alkoxides or halides), aluminum alkyl halides, and aluminum alkyls or aluminum alkyl hydrides.[6,10,12−14] Typically, the carboxylic acids, which are provided as mixtures of isomers from petrochemical plants (octanoic, versatic, naphthenoic acids), carry solubilizing aliphatic substituents R. They are treated with the alkylaluminum reagents to generate the active catalysts in situ (Scheme 1).

Although heterobimetallic complexes with alkylated rare-earth metal centers have been proposed to promote 1,3-diene polymerization via an allyl insertion mechanism, details of the polymerization mechanism and of the structure of the catalytically active center(s) are still elusive.[15−20] Moreover, until now, the interaction of the "cationizing" chloride-donating reagent with alkylated rare-earth metal centers is not well-understood.[21,22] Noteworthy, similar binary and ternary Ln(III)-based Ziegler catalysts also exhibit good initiation activity toward alkylene oxides (oxiranes), styrene, and acetylene.[2,4,8,9] Recently, we and others found that rare-earth metal centers provide a unique stereoelectronic environment for studying structure−activity relationships in Ziegler-type catalysts. For example, the interaction of simple aluminum alkyls ($AlMe_3$ [TMA], $AlEt_3$ [TEA], $AliBu_3$) with industrially relevant *O*-only-bonded rare-earth metal components such as alkoxide, aryloxide, and carboxylate complexes revealed a fundamental reactivity pattern and bonding features.[20,23−29] In the course of the examination of the binary system $\{Ln(O_2CC_6H_2iPr_3\text{-}2,4,6)_3\}_n/AlMe_3$ we discovered an unprecedented alkylation of the Ln center, i.e., a

(12) Porri, L.; Ricci, G.; Shubin, N. *Macromol. Symp.* **1998**, *128*, 53.
(13) Oehme, A.; Gebauer, U.; Gehrke, K.; Beyer, P.; Hartmann, B.; Lechner, M. D. *Macromol. Chem. Phys.* **1994**, *195*, 3773.
(14) Yunlu, K.; He, M.; Cuif, J.-P.; Alas, M. U.S. Patent 6,111,082, 2000.
(15) Taube, R.; Maiwald, S.; Sieler, J. *J. Organomet. Chem.* **2001**, *621*, 327, and references therein.
(16) (a) Kaita, S.; Hou, Z.; Wakatsuki, Y. *Macromolecules* **1999**, *32*, 9078. (b) Kaita, S.; Hou, Z.; Wakatsuki, Y. *Macromolecules* **2001**, *34*, 1539.
(17) (a) Kwag, G.; Lee, H.; Kim, S. *Macromolecules* **2001**, *34*, 5367. (b) Sabirov, Z. M.; Minchenkova, N. K.; Monakov, Y. B. *Vysokomol. Soedin., Ser. B* **1990**, *11*, 803. (c) Porri, L.; Ricci, G.; Giarrusso, A.; Shubin, N.; Lu, Z. *ACS Symp. Ser.* **2000**, *749*, 15.
(18) (a) Shen, Z.; Ouyang, J.; Wang, F.; Hu, Z.; Fu, Y.; Qian, B. *J. Polym. Sci.: Polym. Chem. Ed.* **1980**, *18*, 3345. (b) Rafikov, S. R.; Monakov, Y. B.; Bieshev, Y. K.; Valitova, I. F.; Murinov, Y. I.; Tolstikov, G. A.; Nikitin, Y. E. *Dokl. Akad. Nauk SSSR* **1976**, *229*, 1174.
(19) Kwag, G. *Macromolecules* **2002**, *35*, 4875.
(20) Friebe, L.; Nuyken, O.; Windisch, H.; Obrecht, W. *Macromol. Chem. Phys.* **2002**, *203*, 1055.
(21) Monakov, Y. B.; Sabirov, Z. M.; Urazbaev, V. N.; Efimov, V. P. *Kinet. Catal.* **2001**, *42*, 310.
(22) (a) Evans, W. J.; Champagne, T. M.; Giarikos, D. G.; Ziller, J. W. *Organometallics* **2005**, *24*, 570. (b) Evans, W. J.; Champagne, T. M.; Ziller, J. W. *Organometallics* **2005**, *24*, 4882. (c) Evans, W. J.; Champagne, T. M.; Ziller, J. W. *Chem. Commun.* **2005**, 5925.
(23) (a) Evans, W. J.; Boyle, T. J.; Ziller, J. W. *J. Am. Chem. Soc.* **1993**, *115*, 5084. (b) Evans, W. J.; Greci, M. A.; Ziller, J. W. *Inorg. Chem.* **1998**, *37*, 5221, and references therein.
(24) Biagini, P.; Lugli, G.; Abis, L.; Millini, R. *J. Organomet. Chem.* **1994**, *474*, C16.
(25) (a) Gromada, J.; Mortreux, A.; Chenal, T.; Ziller, J. W.; Leising, F.; Carpentier, J.-F. *Chem. Eur. J.* **2002**, *8*, 3773. (b) Gromada, J.; Mortreux, A.; Nowogrocki, G.; Leising, F.; Mathivet, T.; Carpentier, J.-F. *Eur. J. Inorg. Chem.* **2004**, 3247, and references therein.
(26) (a) Gordon, J. C.; Giesbrecht, G. R.; Brady, J. T.; Clark, D. L.; Keogh, D. W.; Scott, B. L.; Watkin, J. G. *Organometallics* **2001**, *20*, 127. (b) Giesbrecht, G. R.; Gordon, J. C.; Brady, J. T.; Clark, D. L.; Keogh, D. W.; Michalczyk, R.; Scott, B. L.; Watkin, J. G. *Eur. J. Inorg. Chem.* **2002**, 723. (c) Giesbrecht, G. R.; Gordon, J. C.; Clark, D. L.; Scott, B. L.; Watkin, J. G.; Young, K. J. *Inorg. Chem.* **2002**, *41*, 6372.
(27) Fischbach, A.; Herdtweck, E.; Anwander, R.; Eickerling, G.; Scherer, W. *Organometallics* **2003**, *22*, 499.
(28) (a) Evans, W. J.; Giarikos, D. G.; Ziller, J. W. *Organometallics* **2001**, *20*, 5751. (b) Evans, W. J.; Giarikos, D. G. *Macromolecules* **2004**, *37*, 5130.
(29) Evans, W. J.; Giarikos, D. G.; Allen, N. T. *Macromolecules* **2003**, *36*, 4256.

Chart 1. Carboxylic Acids Used in This Study

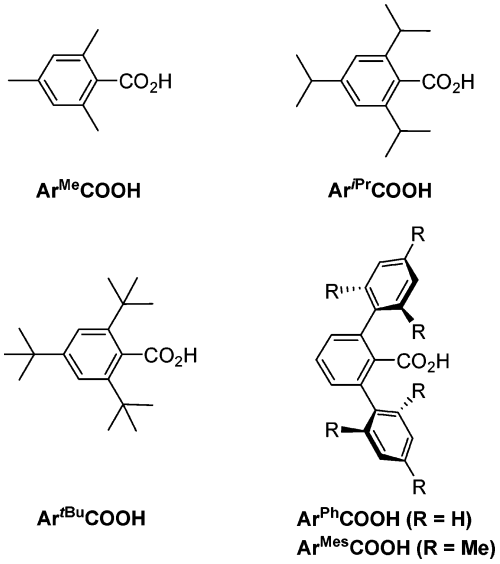

$[O_2CAr^{iPr}] \rightarrow [AlMe_4]$ transformation, and the formation of Me_2-Al-bridged bis(carboxylate) chelating ligands.[30]

Here we wish to present a full account of a detailed investigation of the structure−reactivity relationships of the neodymium carboxylate-based polymerization of isoprene. Tailor-made lanthanide carboxylates were synthesized and reacted with alkylaluminum reagents in order to isolate alkylated bimetallic complexes as possible intermediates in the formation of the active species.

Results and Discussion

Tailor-made Lanthanide Carboxylates with Bulky Benzoate Ligands. Lanthanide carboxylate complexes, which are used in the industrial-scale polymerization of butadiene and isoprene, are generally derived from octanoic, versatic, and naphthenonic acids (Scheme 1). Due to their large "aliphatic tails", they impart enhanced solubility of the corresponding complexes in hexane or heptane solutions. Addition of alkylating reagents, such as trialkylaluminum reagents AlR_3, produces even more soluble components; however, such oily products exhibit a low crystallization tendency and NMR spectra that are extremely difficult to interpret. Therefore, we decided to investigate the alkylation behavior of tailor-made carboxylates derived from sterically demanding, symmetrically substituted aromatic benzoic acids (Chart 1).

All of the lanthanide carboxylates were synthesized according to silylamine elimination reactions from bis(trimethylsilyl)amide complexes $Ln[N(SiMe_3)_2]_3$ (Ln = Y, La, Nd, Gd, Lu)[31] and 3 equiv of the corresponding benzoic acid (Scheme 2).[32] The carboxylate complexes formed in THF solutions at ambient temperature overnight and were isolated by evaporating the solvent in vacuo. After several hexane washings homoleptic carboxylates $\{Ln(O_2CAr^{Me})_3\}_x$ (**1**) and $\{Ln(O_2CAr^{iPr})_3\}_x$ (**2**) were isolated in quantitative yields. Complexes **1** and **2** are insoluble in aliphatic and aromatic solvents, but can be crystallized from donor solvents such as THF, DMSO, and pyridine. Carboxylates $\{Ln(O_2CAr^{tBu})_3(THF)\}_x$ (**3**), $\{Ln(O_2CAr^{Ph})_3(THF)\}_x$ (**4**), and $\{Ln(O_2CAr^{Mes})_3(THF)\}_x$ (**5**) formed mono-THF adducts, as indicated by elemental analysis and ^1H and ^{13}C NMR spectroscopy.

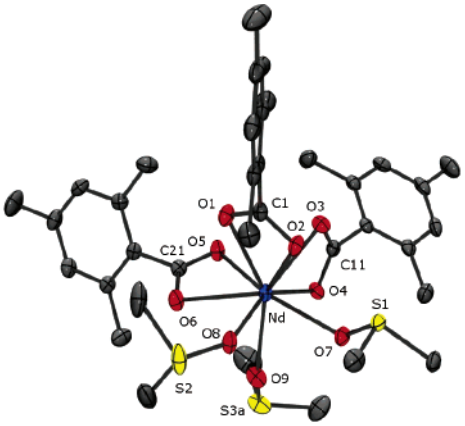

Figure 1. Molecular structure of $[Nd(O_2CC_6H_2Me\text{-}2,4,6)_3(DMSO)_3]$ (**1c′**), with atomic displacement parameters at the 50% probability level. The disorder over two positions at one of the DMSO molecules (S3a, S3b) and all of the hydrogen atoms were omitted for clarity.

Scheme 2. Synthesis of Lanthanide Carboxylates via Silylamine Elimination

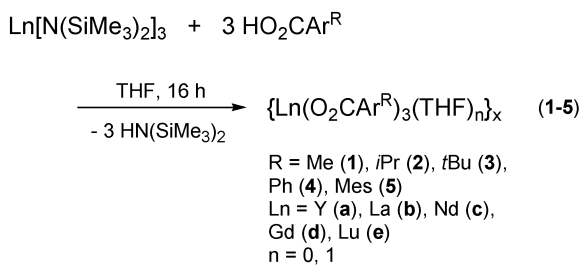

Structural Aspects of Carboxylate Complexes 1b and 1c. Crystallization of complexes **1b** and **1c** from saturated DMSO solutions by slow evaporation of the solvent at ambient temperature yielded X-ray suitable single crystals of mono- (Ln = Nd (**1c′**)) and dinuclear carboxylate complexes (Ln = La (**1b′**)) within several weeks.

The molecular structure of the neodymium derivative $[Nd(O_2CC_6H_2Me_3\text{-}2,4,6)_3(DMSO)_3]$ (**1c′**) is shown in Figure 1, and selected bond distances and angles are listed in Table 1. The nine-coordinate neodymium cation is surrounded by three η^2-coordinated carboxylate ligands and three DMSO molecules in a facial coordination geometry. To the best of our knowledge, **1c′** represents the first mononuclear rare-earth metal carboxylate complex.[33] The carboxylic oxygens of the bidentate benzoate ligands form relatively long and nearly equal Nd−O bond lengths in the range of 2.488(2)−2.551(2) Å. For comparison, the Nd−O bond distances of the terminally coordinated carboxylate ligands in dinuclear $\{Nd[O_2CCH(Ph)Et]_3[HO_2CCH(Ph)Et]_2\}_2$ and $Nd_2[O_2CC(CH_3)_2CH_2CH_3]_6(pyridine)_4$ range from 2.538(2) to 2.549(2) Å and from 2.494(3) to 2.545(3) Å, respectively.[28] On the other hand, the three DMSO molecules show shorter Nd−O bond distances of 2.452(2)−2.480(1) Å.

Driven by the increased steric unsaturation of the larger metal center, the corresponding lanthanum derivative crystallized from DMSO as a dinuclear complex featuring two terminal and one bridging carboxylate ligand per lanthanum atom. Both lantha-

(30) (a) Fischbach, A.; Perdih, F.; Sirsch, P.; Scherer, W.; Anwander, R. *Organometallics* **2002**, *21*, 4569. (b) Fischbach, A. Ph.D. Thesis, Technische Universität München, 2003.

(31) Bradley, D. C.; Ghotra, J. S.; Hart, F. A. *J. Chem. Soc., Dalton Trans.* **1973**, 1021.

(32) Spino, C.; Clouston, L. L.; Berg, D. J. *Can. J. Chem.* **1997**, *75*, 1047.

(33) Ouchi, A.; Suzuki, Y.; Ohki, Y.; Koizumi, Y. *Coord. Chem. Rev.* **1988**, *92*, 29.

Table 1. Selected Bond Lengths and Angles for $[La_2(O_2CC_6H_2Me_3\text{-}2,4,6)_6](DMSO)_4$ (1b′) and $[Nd(O_2CC_6H_2Me_3\text{-}2,4,6)_3](DMSO)_3$ (1c′)

	1b′ (Ln = La)	**1c′** (Ln = Nd)
	Bond Lengths (Å)	
Ln−O1	2.605(1)	2.511(2)
Ln−O2	2.609(1)	2.526(1)
Ln−O3	2.568(2)	2.488(2)
Ln−O4	2.521(1)	2.532(2)
Ln−O4′	2.710(2)	
Ln−O5	2.508(2)	2.551(2)
Ln−O6	2.622(2)	2.524(2)
$Ln-O1_{DMSO}$	2.459(2)	2.452(2)
$Ln-O2_{DMSO}$	2.502(2)	2.468(2)
$Ln-O3_{DMSO}$		2.480(1)
O1−C1	1.257(3)	1.264(3)
O2−C1	1.265(3)	1.262(3)
O3−C11	1.250(3)	1.260(3)
O4−C11		1.262(2)
O4−C11′	1.282(3)	
O5−C21	1.266(3)	1.259(3)
O6−C21	1.268(3)	1.263(2)
	Bond Angles (deg)	
O1−Ln−O2	50.15(5)	52.09(5)
O3−Ln−O4	117.80(5)	52.11(5)
O3−Ln−O4′	49.41(5)	
O4−La−O4′	68.66(5)	
O5−Ln−O6	51.09(6)	51.49(5)
O1−C1−O2	122.4(2)	122.2(2)
O3−C11−O4		122.0(2)
O3−C11−O4′	121.6(3)	
O5−C21−O6	121.9(2)	121.9(2)

num centers are nine-coordinated, involving seven carboxylate oxygen atoms and two DMSO oxygen atoms each. The ORTEP plot of $[La(O_2CC_6H_2Me_3\text{-}2,4,6)_2(\mu\text{-}O_2CC_6H_2Me_3\text{-}2,4,6)(DMSO)_2]_2$ (**1b′**) is shown in Figure 2. Selected intramolecular bond distances and angles are presented in Table 1.

Compared to the neodymium complex **1c′**, the La−O bond distances of 2.508(2)−2.622(2) Å of the η^2-coordinated terminal carboxylate ligands are slightly elongated. The bond lengths match the corresponding values in $La_2[O_2CC(CH_3)_2CH_2CH_3]_6(pyridine)_4$ (2.517(2)−2.625(2) Å).[28] A $\mu_2,\eta^1{:}\eta^2$-coordination mode is realized by both bridging carboxylate ligands, with two short (2.521(1)−2.568(2) Å, η^2) and one long La−O distance (2.710(2) Å, η^1). Similar structural features were previously reported for the dinuclear carboxylate complexes $[La(C_5H_3O_3)_3(H_2O)_2]_2$[34a] and $[La_2(O_2CC_6H_5)_6(C_{12}H_8N_2)_2]$.[34b]

Dialkylaluminum Carboxylate Complexes $[R'_2Al(\mu\text{-}O_2CAr^R)]_2$. To identify any Ln → Al carboxylate ligand transfer by NMR spectroscopy, we initially examined the reaction of AlR_3 with substituted benzoic acids. Dialkylaluminum carboxylates have been reported as major products from the reaction of trialkylaluminum reagents with carboxylic acids.[35] These products are liquids or oily compounds at ambient temperature and were characterized without X-ray crystallographic methods.[36] In 1997 Bethley et al. synthesized a variety of di-*tert*-butylaluminum carboxylates as model compounds for carboxylate alumoxanes $[Al(O)_x(OH)_y(O_2CR)_z]_n$.[37]

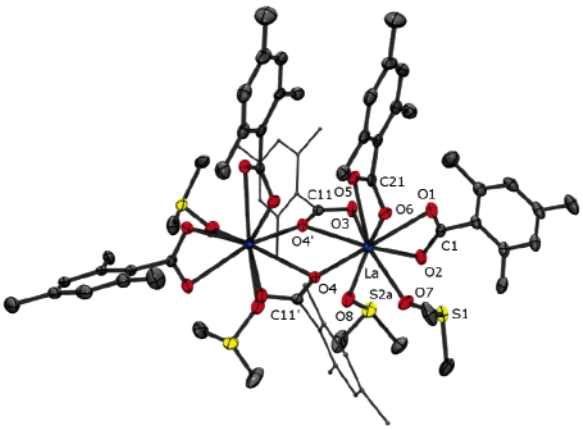

Figure 2. Molecular structure of $[La(O_2CC_6H_2Me_3\text{-}2,4,6)_2(\mu\text{-}O_2CC_6H_2Me_3\text{-}2,4,6)(DMSO)_2]_2$ (**1b′**), with atomic displacement parameters at the 50% probability level. The disorder over two positions at one of the two DMSO molecules (S2a, S2b) and all of the hydrogen atoms were omitted for clarity.

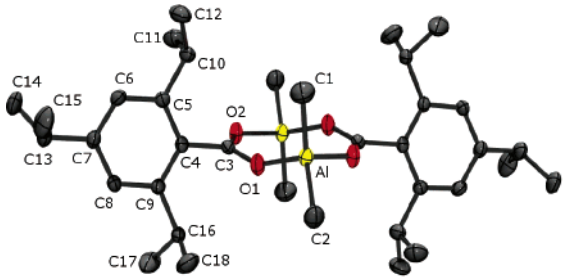

Figure 3. Molecular structure of $[Me_2Al(\mu\text{-}O_2CAr^{iPr})]_2$ (**7**), with atomic displacement parameters at the 50% probability level. Hydrogen atoms were omitted for clarity.

In the course of our studies we reacted trimethyl- and triethylaluminum with all of the aromatic carboxylic acids shown in Chart 1. Equimolar 1:1 reaction mixtures gave crystalline products **6**−**11** of composition "$R'_2Al(\mu\text{-}O_2CAr^R)$" (R′ = Me, Et) in quantitative yields after 2 h (eqs 1, 2).

$$AlMe_3 + Ar^RCO_2H \rightarrow 1/2\,[Me_2Al(\mu\text{-}O_2CAr^R)]_2\ (\mathbf{6}\text{−}\mathbf{10}) + CH_4 \quad (1)$$

R = Me (**6**), *i*Pr (**7**), *t*Bu (**8**), Ph (**9**), Mes (**10**)

$$AlEt_3 + Ar^{iPr}CO_2H \rightarrow 1/2\,[Et_2Al(\mu\text{-}O_2CAr^{iPr})]_2\ (\mathbf{11}) + C_2H_6 \quad (2)$$

Compounds **6**−**11** were fully characterized by elemental analysis and IR and NMR spectroscopy. The ambient-temperature ^1H NMR spectra of **6**−**10** exhibit only one signal in the alkylaluminum region for the dimethylaluminum units (−0.23 to −1.05 ppm). Recrystallization of **7** from saturated hexane solutions yielded colorless single crystals suitable for an X-ray structure analysis. The solid-state structure of **7** is shown in Figure 3, and relevant bond lengths and angles are presented in Table 2.

As predicted previously for other alkylaluminum carboxylates from IR and Raman spectroscopy, mass spectrometry, and molecular weight measurements[36] and as proven for $[tBu_2Al$-

(34) (a) Li, X.; Chen, X.-A.; Zhao, L.; Chen, B.-M. *Acta Crystallogr. C* **1997**, *53*, 1015. (b) Shi, Q.; Hu, M.; Cao, R.; Liang, Y.; Hong, M. *Acta Crystallogr. E* **2001**, *57*, m122.

(35) Eisch, J. J. In *Comprehensive Organometallic Chemistry*; Wilkinson, G., Stone, F. G. A., Abel, E. W., Eds.; Pergamon Press: Oxford, U.K., 1988; Vol. 1, Chapter 6.

(36) (a) Weidlein, J. *Z. Anorg. Allg. Chem.* **1970**, *378*, 245. (b) Pietrzykowski, A.; Pasynkiewicz, S.; Poplawaska, J. *Main Group Met. Chem.* **1966**, *18*, 651. (c) Kolesnikov, G. S.; Davidova, S. L.; Yampolskaya, M. A.; Klimentova, N. V. *Bull. Acad. Sci. USSR (Engl. Transl.)* **1962**, 783. (d) Zakharkin, L. J.; Kolesnikov, G. S.; Davidova, S. L.; Gavrilenko, V. V.; Kamyshova, A. A. *Bull. Acad. Sci. USSR (Engl. Transl.)* **1961**, 336. (e) Zenina, G. V.; Sheverdina, N. I.; Kocheskov, K. A. *Proc. Acad. Sci. USSR (Engl. Transl.)* **1970**, *195*, 786.

(37) Bethley, C. E.; Aitken, C. L.; Harlan, C. J.; Koide, Y.; Bott, S. C.; Barron, A. R. *Organometallics* **1997**, *16*, 329.

Table 2. Selected Bond Lengths and Angles for $[Me_2Al(\mu\text{-}O_2CC_6H_2iPr_3\text{-}2,4,6)]_2$ (7)

Bond Lengths (Å)			
Al−C1	1.941(2)	Al−O2′	1.840(1)
Al−C2	1.935(2)	O1−C3	1.261(2)
Al−O1	1.810(1)	O2−C3	1.256(2)
Bond Angles (deg)			
O1−Al−C1	108.21(7)	O2′−Al−C1	107.35(7)
O1−Al−C2	107.47(7)	O2′−Al−C2	104.65(7)
O1−Al−O2′	104.71(5)	O1−C3−O2	122.4(1)
C1−Al−C2	123.02(9)		

Scheme 3. Synthesis of Heterobimetallic Lanthanide Carboxylates 12a−e via Alkylation with TMA

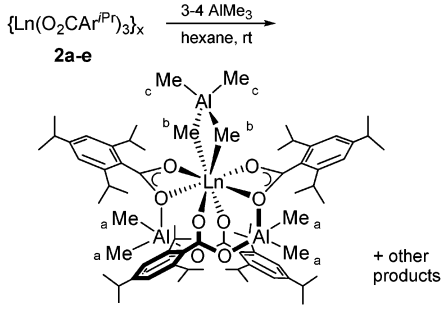

Ln = Y (**12a**), La (**12b**), Nd (**12c**), Gd (**12d**), Lu (**12e**)

(μ-O_2CR)]$_2$ by X-ray structural investigations,[37] **7** crystallized as a centrosymmetric dimer with two Me_2Al units bridged by two bidentate carboxylate groups. The aluminum atoms of the central eight-membered ring are four-coordinated by two carbon and two oxygen atoms in a tetrahedral fashion with Al−O bond lengths (1.810(1), 1.840(1) Å) consistent with this coordination number.[38] On the other hand Al−C bond lengths of 1.935(2)−1.941(2) Å are in agreement with similar dimethylaluminum alkoxides (e.g., $[Me_2Al(\mu\text{-}OCMe_2Ph)]_2$:[39] 1.9415(9)−1.9456(9) Å) and aryloxides (e.g., $Me_2Al(OC_6H_2tBu_2\text{-}2,6\text{-}Me\text{-}4(pyridine)$:[40] 1.964(6)−1.956(6) Å).

Carboxylate−Alkyl Exchange in $\{Ln(O_2CAr^{iPr})_3\}_x$. All of the synthesized homoleptic lanthanide carboxylates were reacted with trimethyl- and triethylaluminum. For the isopropyl-substituted $\{Ln(O_2CAr^{iPr})_3\}_x$ (**2a−e**) slow addition of a slight excess of trimethylaluminum (TMA, 3−4 equiv) to a hexane suspension yielded hexane-insoluble (Ln = Y, Lu) or hexane-soluble (Ln = La, Nd, Gd) Ln−Al heterobimetallic complexes **12a−e** in moderate isolated yields of 35−45% (Scheme 3). Up to now a detailed investigation of the byproducts failed due to their similar solubilities in aliphatic and aromatic solvents. According to the ^{1}H NMR spectra of the crude reaction mixtures, at least three different alkylated byproducts formed; however, homoleptic tetramethylaluminate complexes $Ln[(\mu\text{-}Me)_2AlMe_2]_3$ were not observed.[41]

The hexane-insoluble yttrium (**12a**) and lutetium derivatives (**12e**) have been isolated from the reaction mixture after 24 h via centrifugation. After several washings with hexane and drying under vacuum a net composition of the products of $[LnAl_3Me_8(O_2CC_6H_2iPr_3\text{-}2,4,6)_4]$ was indicated by elemental analysis and IR and NMR spectroscopy. At ambient temperature the proton NMR spectra of **12a** showed one set of signals for the carboxylate ligands and two peaks in the aluminum alkyl region with an integral ratio of 12:12 (−0.08 (a, Scheme 3) and −0.41 ppm (b/c, Scheme 3)). At lower temperature, the higher-field-shifted aluminate resonance separated into two well-resolved signals at −0.17 (c) and −0.80 (b) ppm (193 K, toluene-d_8), attributable to bridging and terminal methyl groups. Due to broad signals, no ^{89}Y coupling was observable. A decoalescence temperature of 263 K was determined for the yttrium derivative.

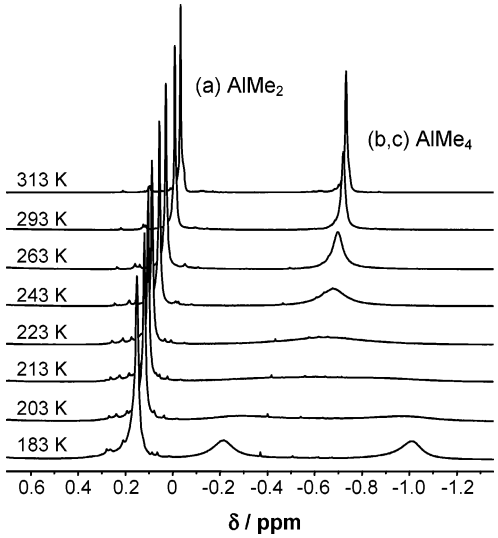

Figure 4. Region of the variable-temperature ^{1}H NMR spectra of **12b** measured in toluene-d_8 (cf. Scheme 3).

Under similar reaction conditions the larger metal centers lanthanum, neodymium, and gadolinium formed readily hexane-soluble heterobimetallic complexes within minutes (La (**12b**), Nd (**12c**)) to hours (Gd (**12d**)). After TMA addition the carboxylate hexane suspensions turned clear and the products had to be separated by repeated crystallization from saturated hexane solutions at −45 °C. Elemental analysis and proton and carbon NMR spectra revealed the formation of products of net composition $[LnAl_3Me_8(O_2CC_6H_2iPr_3\text{-}2,4,6)_4(hexane)]$. One molecule of hexane entrapped in the crystal lattice could not be removed under reduced pressure ($\sim 10^{-2}$ mbar). Also, the proton NMR spectrum of **12b** shows only one set of signals at 298 K for the carboxylate ligands and a 12:12 ratio of the two alkylaluminum resonances (0.13 (a, Scheme 3) and −0.62 ppm (b/c, Scheme 3)). A decoalescence temperature of 213 K, as obtained from variable-temperature NMR experiments in toluene-d_8 (Figure 4), is consistent with an increased steric unsaturation and more rapid alkyl exchange at the larger lanthanum center compared to the smaller yttrium derivative **12a**.

The results of the dynamic NMR experiments of complexes **12a** and **12b** are presented in Figures 4 and 5 and Table 3. For the yttrium derivative **12a**, the aluminate methyl group exchange proceeds with activation parameters $\Delta H^{\ddagger} = 73(4)$ kJ mol^{-1} and $\Delta S^{\ddagger} = 66(3)$ J K^{-1} mol^{-1}, consistent with a strongly bonded aluminate ligand and a *dissociative* methyl group exchange (Figure 5) reported earlier for Al_2Me_6.[42]

In contrast, an *associative* methyl group exchange is indicated by $\Delta S^{\ddagger} = -58(3)$ J K^{-1} mol^{-1} for the lanthanum derivative **12b**, as proposed previously for half-metallocene bis(tetra-

(38) Haaland, A. *Coordination Chemistry of Aluminum*; Robinson, G. H., Ed.; VCH: New York, 1993; Chapter 1.

(39) Allan, J. F.; Clegg, W.; Elsegood, M. R. J.; Henderson, K. W.; McKeown, A. E.; Moran, P. H.; Rakov, I. M. *J. Organomet. Chem.* **2000**, *602*, 15.

(40) Healy, M. D.; Ziller, J. W.; Barron, A. R. *J. Am. Chem. Soc.* **1990**, *112*, 2949.

(41) Evans, W. J.; Anwander, R.; Ziller, J. W. *Organometallics* **1995**, *14*, 1107.

(42) O'Neill, M. E.; Wade, K. In *Comprehensive Organometallic Chemistry*; Wilkinson, G., Stone, F. G. A., Abel, E. W., Eds.; Pergamon Press: New York, 1982; p 593.

Table 3. Thermodynamic Data for the Exchange of Bridging and Terminal Methyl Groups in Ln−Al Heterobimetallic Complexes 12a and 12b

complex	T_c[a] [K]	$\Delta G^{\ddagger}$[b] [kJ mol^{-1}]	$\Delta H^{\ddagger}$[b] [kJ mol^{-1}]	$\Delta S^{\ddagger}$[b] [J K^{-1} mol^{-1}]
12a (Ln = Y)	263	53(3)	73(4)	66(3)
12b (Ln = La)	213	45(2)	28(2)	−58(3)
$Me_2Al(\mu\text{-}Me)_2AlMe_2$[c]		44.8	81.5	123.1
$Me_2Si(2\text{-}MeBenzInd)_2Y[(\mu\text{-}Me)_2AlMe_2]$[c]		63.0	24.3	−130

[a] Decoalescence temperature. [b] Extracted by line shape analysis. Uncertainities mainly based on temperature errors. [c] Provided for comparison (from refs 42, 43).

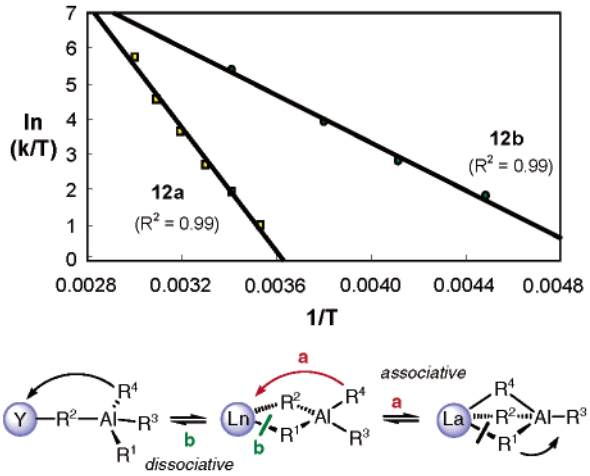

Figure 5. Arrhenius plot and proposed exchange mechanism for the exchange of bridging and terminal methyl groups in Ln−Al heterobimetallic complexes **12a** and **12b**.

Scheme 4. Synthesis of Heterobimetallic Lanthanide Carboxylates 13 via Alkylation with TEA

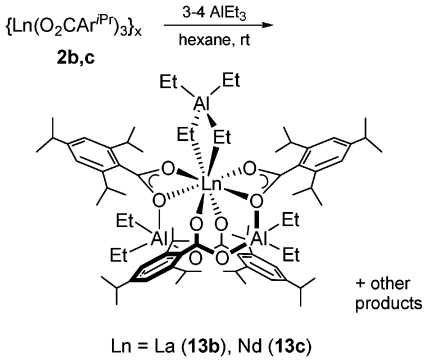

methylaluminate) complexes and C_2-symmetric *ansa*-yttrocene complex $Me_2Si(2\text{-}MeBenzInd)_2Y[(\mu\text{-}Me)_2AlMe_2]$.[43] Moreover, a relatively weak aluminate bonding is proposed by $\Delta H^{\ddagger} = 28(2)$ kJ mol^{-1} for the large rare-earth metal center lanthanum. Note that the larger rare-earth metal centers, and in particular neodymium, are known to display enhanced catalytic activity in Ziegler-type catalysts. The comparatively increased activation enthalpy $\Delta(\Delta G^{\ddagger})$ of ca. 8 kJ mol^{-1} for the smaller metal center yttrium corresponds to a slowing of the methyl group exchange by a factor of 5×10^{-2} at ambient temperature.

Similar products were obtained in the reaction of **2b** and **2c** with 3−4 equiv of triethylaluminum (TEA) in hexane at ambient temperature (Scheme 4). After 6 h the mixtures were filtrated and the supernatants dried in vacuo. The highly soluble heterobimetallic lanthanide carboxylates **13b** (Ln = La) and **13c** (Ln = Nd) were isolated in yields of 34 and 17% by crystallization at −45 °C for several days. In the case of the smaller metal centers Y and Lu no alkylated products were isolated.

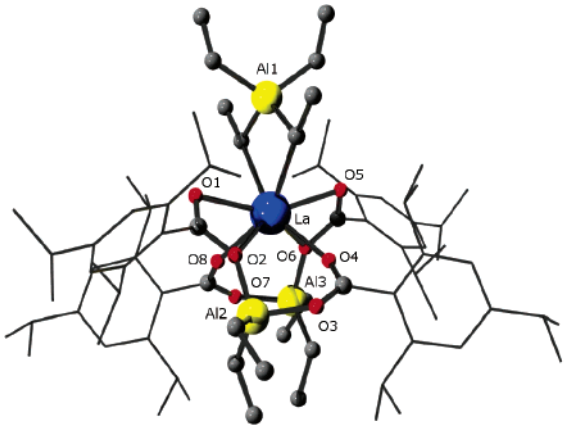

Figure 6. Ball-and-stick diagram showing the central core of **13b**.

Also for the TEA-alkylation products, elemental analysis and NMR spectroscopic data confirmed the formation of complexes **13** with a net composition $[LnAl_3Et_8(O_2CC_6H_2iPr_3\text{-}2,4,6)_4\text{-}(hexane)]$. The proton NMR spectrum of **13b** showed two different aluminum ethyl groups in a 1:1 ratio at ambient temperature, consistent with two bridging diethylaluminum groups and one highly fluctuating tetraethylaluminate unit. Despite the different coordination modes of the carboxylate ligands (η^1, η^2), only one set of signals is realized for the isopropyl-substituted benzoate ligands in the ^{1}H and ^{13}C NMR spectra.

Recrystallization of complex **13b** from a saturated hexane solution yielded single crystals suitable for an X-ray structure analysis. Due to severe disordering of the highly mobile isopropyl groups, even at low temperatures, the connectivity of the central core of **13b** is presented as a ball-and-stick model (Figure 6). The solid-state structure, which is related to the previously reported TMA-alkylated neodymium derivative **12c** (triclinic, space group $P\bar{1}$),[30a] shows an eight-coordinated lanthanum atom. One η^2-coordinating tetraethylaluminate unit and six oxygen atoms of two $AlMe_2$-linked bis(carboxylate) ligands accomplish an inner coordination sphere of local C_2 symmetry.

In the course of our investigations we developed three alternative routes to synthesize the heterobimetallic carboxylates **12a**−**e**, all of them starting with homoleptic tetramethylaluminates $Ln[(\mu\text{-}Me)_2AlMe_2]_3$. As presented for the yttrium derivative in eqs 3−6, the hexane-insoluble alkylated isopropyl carboxylate **12a** was isolated from the reaction of $Y(AlMe_4)_3$ with either the dimethylaluminum carboxylate $[Me_2Al(\mu\text{-}O_2\text{-}CAr^{iPr})]_2$ (**7**) (eq 4), the carboxylic acid HO_2CAr^{iPr} (eq 5), or the homoleptic carboxylate $\{Y(O_2CAr^{iPr})_3\}_x$ (**2a**) (eq 6). Yields and product distributions can be directly compared with the alkylation of the donor-free carboxylate **2a** (eq 3, Scheme 3).

(43) (a) Eppinger, J. Ph.D. Thesis, Technische Universität München, 1999. (b) Anwander, R.; Klimpel, M. G.; Dietrich, H. M.; Shorokhov, D. J.; Scherer, W. *Chem. Commun.* **2003**, 1008.

Due to an efficient precipitation of the hexane-insoluble product from the reaction of readily soluble educts, pathway 4 was used to synthesize larger amounts of analytically pure **12a** within 2−4 h.

$$\{Y(O_2CAr^{iPr})_3\}_x\ (\mathbf{2a}) + 4\ AlMe_3 \rightarrow \mathbf{12a} + \text{other products} \quad (3)$$

$$Y(AlMe_4)_3 + 2\ [Me_2Al(\mu\text{-}O_2CAr^{iPr})]_2\ (\mathbf{7}) \rightarrow \mathbf{12a} + \text{other products} \quad (4)$$

$$Y(AlMe_4)_3 + 4\ HO_2CAr^{iPr} \rightarrow \mathbf{12a} + \text{other products} \quad (5)$$

$$Y(AlMe_4)_3 + \{Y(O_2CAr^{iPr})_3\}_x\ (\mathbf{2a}) \rightarrow \mathbf{12a} + \text{other products} \quad (6)$$

Alkylation of $\{Ln(O_2CAr^{Me})_3\}_x$ and $\{Ln(O_2CAr^{tBu})_3\}_x$ with TMA. The formation of complexes $Ln[(O_2CAr^{iPr})_2(\mu\text{-}AlR_2)]_2[(\mu\text{-}R)_2AlR_2]$ (**12**, R = Me; **13**, R = Et) as alkylation products seems to be intrinsically associated with isopropyl-substituted benzoate ligands. Several attempts to synthesize similar, alkylated, heterobimetallic lanthanide carboxylates bearing methyl, *tert*-butyl, phenyl, or mesityl derivatives produced lower or higher alkylated products instead. In the case of the sterically less crowded methyl derivatives $\{Ln(O_2CAr^{Me})_3\}_x$ (**1**) the reaction with excess TMA did not produce any larger amounts of alkylated products overnight. Nevertheless, one of the above-mentioned alternative syntheses using $Ln(AlMe_4)_3$ as a precursor succeeded in the formation of a new type of homoleptic mixed-metal carboxylate. According to eq 7 slow addition of 3 equiv of dimethylaluminum carboxylate **6** to a toluene solution of homoleptic tetramethylaluminate yielded a white suspension, which was stirred at ambient temperature for 18 h. Centrifugation and repeated extraction of the solid into toluene yielded two soluble compounds, as indicated by proton NMR spectroscopy. Unfortunately, separation of the alkylated products **14a** and **14b** from the nonreacted **6** failed due to similar solubility in aromatic solvents. However, ^1H and ^{13}C NMR spectra suggest the formation of a lanthanide center that is surrounded by three dimethylaluminum-bridged bis(carboxylate) ligands. Note that two of such in situ formed ancillary ligands were observed in complexes **12** and **13** in the presence of isopropyl-substituted benzoates.

$$Ln(AlMe_4)_3 + 3\ [Me_2Al(\mu\text{-}O_2CAr^{Me})]_2\ (\mathbf{6}) \rightarrow Ln[(O_2CAr^{Me})(\mu\text{-}AlMe_2)(Ar^{Me}CO_2)]_3\ (\mathbf{14}) \quad (7)$$

Ln = Y (**14a**), La (**14b**)

In contrast, alkylation of complexes $\{Ln(O_2CAr^{tBu})_3(THF)\}_x$ (**3**), bearing the sterically more crowded *tert*-butyl-substituted carboxylate ligands, with TMA exclusively produced hexane-soluble products overnight (Scheme 5). Filtration and evaporation of the solvent gave sticky residues, which were washed with small amounts of cold hexane. The purified residues were dried under reduced pressure and identified as "bis-alkylated" complexes **15a**,**b** with net composition $[LnAl_2Me_8(O_2CC_6H_2tBu_3\text{-}2,4,6)]$ by elemental analysis and NMR and IR spectroscopy. The soluble byproducts were investigated by proton NMR spectroscopy, revealing the mere formation of two alkylated products.

To synthesize larger amounts of complexes **15a,b** and the neodymium derivative **15c** in the absence of any byproduct, the "tetramethylaluminate route" was employed. Accordingly,

Scheme 5. Synthesis of Mono(carboxylate)−Bis(tetramethylaluminate) Complexes 15 via the Alkylation of *tert*-Butyl-Substituted Lanthanide Benzoates 3

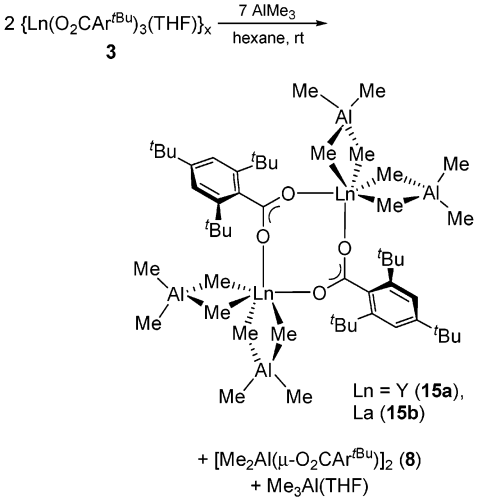

$Ln(AlMe_4)_3$ were reacted with 1 equiv of the carboxylic acid, added as a toluene suspension (eq 8). Instantaneous evolution of methane occurred, and the clear mixture was stirred at ambient temperature for 4 h. After filtration and evaporation of the solvent the alkylated carboxylates **15** were isolated in almost quantitative yields.

$$2\ Ln[(\mu\text{-}Me)_2AlMe_2]_3 + 2\ HO_2CAr^{tBu} \rightarrow \{Ln(O_2CAr^{tBu})[(\mu\text{-}Me)_2AlMe_2]_2\}_2\ (\mathbf{15}) + 2\ CH_4 + 2\ AlMe_3 \quad (8)$$

Ln = Y (**15a**), La (**15b**), Nd (**15c**)

All of the spectroscopic data were in good agreement with the formation of mono(carboxylate)−bis(tetramethylaluminate) complexes $\{Ln(O_2CAr^{tBu})[(\mu\text{-}Me)_2AlMe_2]_2\}_2$ **15a** (Ln = Y), **15b** (Ln = La), and **15c** (Ln = Nd). The ambient-temperature proton NMR spectra of complex **15** showed only one set of signals for the carboxylate ligands and broad resonances for the fluctuating tetramethylaluminate units at −0.12, −0.03, and 9.7 ppm, respectively. The distinct low-field shift for the paramagnetic Nd derivative is in accordance with the 10.5 ppm observed for homoleptic $Nd(AlMe_4)_3$.[41] For the smallest metal center (**15a**: Ln = Y), three well-resolved signals with an integral ratio of 24:12:12 were observed at 183 K, indicating three different types of aluminum-bonded methyl groups. A region of the variable-temperature NMR spectra is presented in Figure 7.

At 268 K the resonance of the initially uniform (interchanging) aluminate methyl groups started to separate into two signals attributable to terminal Al-Me (high-field shifted) and bridging Y-Me-Al methyl groups (low-field shifted). A second decoalescence of the former signal was observed at 228 K, resulting in two well-separated slightly broadened peaks at −0.25 and −0.60 ppm (183 K, 1:1 ratio). Although significant broadening of the low-field shifted signal of the bridging methyl groups was observed at lower temperatures, as indicated by the disappearance of the $^2J_{HY}$ coupling (observable only from 223 to 213 K), a further separation did not occur until 183 K.

Recrystallization of complexes **15** from warm hexane/toluene mixtures yielded single crystals of **15b** and **15c** suitable for an X-ray structure analysis. The ORTEP plot of the neodymium

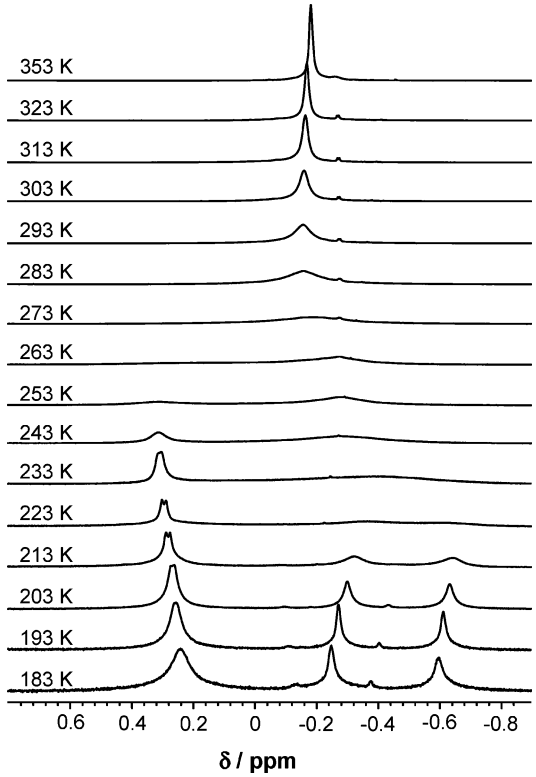

Figure 7. Region of the variable-temperature ^{1}H NMR spectra of **15a** measured in toluene-d_8.

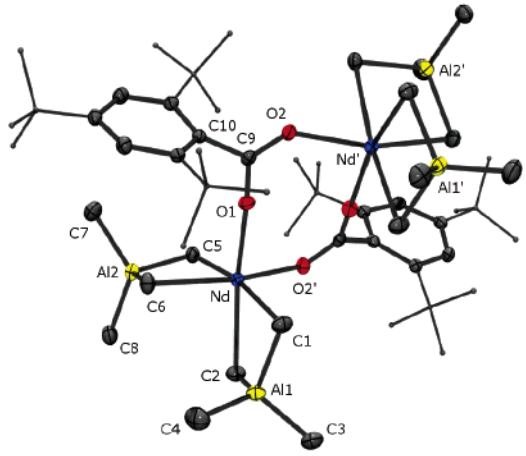

Figure 8. Molecular structure of $\{Nd(O_2CAr^{tBu})[(\mu\text{-}Me)_2AlMe_2]_2\}_2$ (**15c**) with atomic displacement parameters at the 50% probability level. Hydrogen atoms were omitted for clarity.

derivative is shown in Figure 8, and selected intramolecular distances and bond angles of **15b** and **15c** are presented in Table 4.

The solid-state structures of **15b** and **15c** confirm the formation of dimeric molecules with a central eight-membered $\{LnOCO\}_2$ ring involving two bridging carboxylate ligands. Both of the lanthanide cations are six-coordinated by two oxygen atoms of different carboxylate ligands and four methyl groups of the tetramethylaluminate units. The Nd−C(μ) distances of **15c** ranging from 2.614(2) to 2.626(2) Å can be directly compared with the formally five-coordinate heteroleptic amido-substituted neodymium tetramethylaluminate $Nd[NiPr_2][(\mu\text{-}NiPr_2)(\mu\text{-}Me)AlMe_2][(\mu\text{-}Me)_2AlMe_2]$ (2.639(3), 2.659(3) Å).[44]

(44) Evans, W. J.; Anwander, R.; Ziller, J. W. *Inorg. Chem.* **1995**, *34*, 5927.

Table 4. Selected Bond Lengths, Intramolecular Contacts, and Angles for $\{La(O_2CAr^{tBu})[(\mu\text{-}Me)_2AlMe_2]_2\}_2$ (15b) and $\{Nd(O_2CAr^{tBu})[(\mu\text{-}Me)_2AlMe_2]_2\}_2$ (15c)

	15b (Ln = La)	**15c** (Ln = Nd)
	Bond Lengths (Å)	
Ln···Al1	3.255(1)	3.189(1)
Ln···Al2	3.255(1)	3.178(1)
Al1···Al1′	7.700(1)	7.787(1)
Al2···Al2′	9.804(1)	9.922(1)
Ln−O1	2.370(2)	2.282(1)
Ln−O2′	2.434(2)	2.365(1)
Ln−C1	2.681(3)	2.615(2)
Ln−C2	2.679(3)	2.620(2)
Ln−C5	2.693(3)	2.614(2)
Ln−C6	2.693(4)	2.626(2)
Al1−C1	2.070(3)	2.071(2)
Al1−C2	2.063(3)	2.076(2)
Al1−C3	1.962(4)	1.966(3)
Al1−C4	1.969(5)	1.969(3)
Al2−C5	2.072(3)	2.081(3)
Al2−C6	2.066(4)	2.073(2)
Al2−C7	1.971(4)	1.966(3)
Al2−C8	1.971(3)	1.978(2)
C9−O1	1.282(3)	1.276(2)
C9−O2	1.249(3)	1.260(2)
	Bond Angles (deg)	
O1−Ln−O2′	102.93(7)	94.79(5)
C1−Ln−C2	77.28(9)	79.29(7)
C5−Ln−C6	78.1(1)	80.64(7)
C1−Al1−C2	108.2(1)	107.32(9)
C3−Al1−C4	117.8(2)	117.5(1)
C5−Al2−C6	110.1(1)	109.44(9)
C7−Al2−C8	119.6(2)	120.3(1)
O1−C9−O2	120.2(3)	121.1(2)

Slightly shorter Nd−C(μ) bond lengths were observed in homoleptic $Nd[(\mu\text{-}Me)_2AlMe_2]_3$ (av 2.598 Å).[41,45] Due to the bulky carboxylate ligands, the central eight-membered ring is bent, resulting in two different Al−Al′ distances of 7.787(1) and 9.922(1) Å (see Figure 9). The Nd−O bond distances of 2.282(1) and 2.365(1) Å are only slightly shorter than those in other η^1-coordinated (bridged) carboxylate ligands, e.g., in higher coordinated $Nd_2[O_2CC(CH_3)_2CH_2CH_3]_6(pyridine)_4$ (2.360(3)−2.434(3) Å)[28] or $[Nd_2(L\text{-}\alpha\text{-alanine})_4(H_2O)_8](ClO_4)_6$ (2.343(7)−2.464(5) Å).[46]

Due to the larger metal center, all of the La−C and La−O distances in **15b** appear slightly elongated compared to the neodymium derivative **15c**. For comparison, the La−C(μ) bond lengths in six-coordinate $La(NMe_2)_2(GaMe_3)_2(GaMe_4)$[47] and seven-coordinate $La[OSi(OtBu)_3](AlMe_4)_2(AlMe_3)$[48a,b] are in the range 2.742(2)−2.992(5) Å and 2.668(5)−2.798(3) Å, respectively. The La−O bond lengths of 2.370(2) and 2.434(2) Å lie in the range of similar heteroleptic carboxylate complexes, e.g., $La_2[O_2CC(CH_3)_2CH_2CH_3]_6(pyridine)_4$ (av 2.513 Å).[28]

Alkylation of $\{Ln(O_2CAr^{Ph})_3(THF)\}_x$ and $\{Ln(O_2CAr^{Mes})_3(THF)\}_x$ with TMA. Finally, the alkylation behavior of $\{Ln(O_2CAr^{Ph})_3(THF)\}_x$ (**4**) and $\{Ln(O_2CAr^{Mes})_3(THF)\}_x$ (**5**), bearing diphenyl- and dimesityl-substituted carboxylate ligands, was investigated. Addition of an excess of TMA (>7 equiv) to a hexane suspension of the homoleptic lanthanide carboxylates **4**

(45) Klooster, W. T.; Lu, R. S.; Anwander, R.; Evans, W. J.; Koetzle, T. F.; Bau, R. *Angew. Chem., Int. Ed.* **1998**, *37*, 1268.

(46) Glowiak, T.; Legendziewicz, J.; Huskowska, E.; Gawryszenwska, P. *Polyhedron* **1996**, *15*, 2939.

(47) Evans, W. J.; Anwander, R.; Doedens, R. J.; Ziller, J. W. *Angew. Chem., Int. Ed. Engl.* **1994**, *33*, 1641.

(48) (a) Fischbach, A.; Klimpel, M. G.; Widenmeyer, M.; Herdtweck, E.; Scherer, W.; Anwander, R. *Angew. Chem., Int. Ed.* **2004**, *43*, 2234. (b) Fischbach, A.; Eickerling, G.; Scherer, W.; Herdtweck, E.; Anwander, R. *Z. Naturforsch.* **2004**, *59b*, 1353. (c) Dietrich, H. M.; Zapilko C.; Herdtweck, E.; Anwander, R. *Organometallics* **2005**, *24*, 5767.

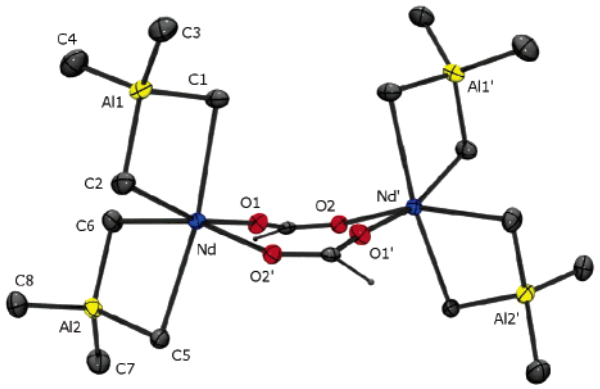

Figure 9. Partial view of $\{Nd(O_2CAr^{tBu})[(\mu\text{-}Me)_2AlMe_2]_2\}_2$ (**15c**).

did not produce any clear solutions overnight. After 18 h the hexane-insoluble solids were separated via centrifugation from the reaction mixtures, washed several times with hexane, extracted into toluene, and dried in vacuo. The collected hexane solutions were evaporated under reduced pressure, yielding sticky solids. Several attempts to isolate a well-defined alkylated product from both the hexane-insoluble and the hexane-soluble part, via crystallization from saturated toluene or hexane solutions, failed due to the similar solubility of the alkylated species. Nevertheless, the formation of the dimethylalumium-bridged cleavage product $[Me_2Al(\mu\text{-}O_2CAr^{Ph})]_2$ (**9**) was unequivocally proven by means of NMR spectroscopy. Additionally, two or three further signals in the alkylaluminum region of the proton NMR spectra of the hexane-insoluble parts were observed for yttrium and lanthanum. In agreement with the identification of **9** the observation of a characteristic doublet at -0.39 ppm ($^2J_{YH} = 2.6$ Hz) for the yttrium derivative points to the formation of lanthanide tetramethylaluminate complexes.

$$\{Ln(O_2CAr^{Ph})_3(THF)\}_x + >7\ AlMe_3 \rightarrow [Me_2Al(\mu\text{-}O_2CAr^{Ph})]_2\ (\mathbf{9}) + Me_3Al(THF) + \text{alkylated Ln products} \quad (9)$$

$$\{Ln(O_2CAr^{Mes})_3(THF)\}_x + >7\ AlMe_3 \rightarrow [Me_2Al(\mu\text{-}O_2CAr^{Mes})]_2\ (\mathbf{10}) + Me_3Al(THF) + \text{alkylated Ln products} \quad (10)$$

Similar problems resulted from the alkylation of dimesityl-substituted carboxylates **5** after an 18 h reaction period. The NMR spectroscopic investigation of the hexane-soluble residues showed the formation of **10** as a cleavage product from the alkylation of the yttrium and lanthanum metal centers. Unfortunately, similar solubility and several signals in the alkylaluminum regions prevented the unequivocal identification of alkylated Ln-containing products.

Attempts to synthesize and isolate one of the alkylation products via alternative strategies failed. However, the "tetramethylaluminate route" using $Ln[(\mu\text{-}Me)_2AlMe_2]_3$ and 1 equiv of HO_2CAr^{Ph} generated hexane-soluble mono(carboxylate)−bis(tetramethylaluminate) complexes **16** similar to complexes **15**, carrying the *tert*-butyl-substituted benzoate ligands (Scheme 6). After a 3 h reaction period the hexane-insoluble parts were separated by centrifugation and the products purified via crystallization.

Elemental analysis and proton and carbon NMR spectroscopy confirmed the formation of complexes **16**. Due to a rapid exchange of terminal and bridging methyl groups, the ambient-temperature ^{1}H NMR spectra showed only one signal for the

Scheme 6. Synthesis of Mono(carboxylate)−Bis(tetramethylaluminate) Complexes 16 via the "Tetramethylaluminate Route"[48]

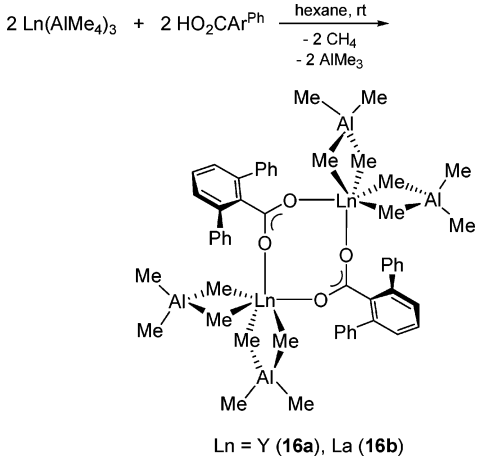

tetramethylaluminate units. In the case of the smaller metal center (Ln = Y; **16a**) four separated signals with an integral ratio of 12:12:12:12 were observed at −80 °C, attributable to two different Y−(μ-Me)−Al (broad signals at 0.15 and −0.53 ppm) and two different Al−Me units (sharp signals at −0.27 and −0.74 ppm).

Carboxylate−Alkyl Exchange. A Mechanistic Scenario of the Formation of Differently Alkylated Ln Carboxylate Complexes. From the results presented above it can be rationalized that not only electronic effects control the formation of differently alkylated products. The steric demand of the aliphatic and aromatic substituents in 2,6-position of the benzoate ligands is also a crucial factor governing the reaction of the homoleptic carboxylates with an excess of alkylaluminum reagents. We propose a mechanistic alkylation scenario as shown in Scheme 7. Accordingly, homoleptic tetramethylaluminate $Ln(AlMe_4)_3$ is a key intermediate (**I$_4$**) for the reassociation reaction with separated dimethylaluminum carboxylates **6**−**10**. The active role of $Ln(AlMe_4)_3$ is supported by the novel "tetraalkylaluminate route", giving access to complexes $[Me_2Al(O_2CC_6H_2iPr_3\text{-}2,4,6)_2]_2Ln[(\mu\text{-}Me)_2AlMe_2]$ (**12** = **I$_6$**), $\{Ln(O_2CC_6H_2tBu_3\text{-}2,4,6)[(\mu\text{-}Me)_2AlMe_2]_2\}_2$ (**15** = **I$_3$**), and $Ln[(O_2CAr^{Me})(\mu\text{-}AlMe_2)(Ar^{Me}CO_2)]_3$ (**14**). Furthermore, $Ln(AlMe_4)_3$ display an extraordinary catalytic activity in the *cis*-1,4 stereospecific polymerization of isoprene.[48a,b]

Stereospecific Polymerization of Isoprene by Binary Ziegler-Type Catalysts. Pre-alkylated Ln−Al heterobimetallic complexes **12**, **13**, and **15** were used as catalyst components in isoprene polymerization. A binary Ziegler-type precatalyst mixture was obtained by addition of various amounts of Et_2AlCl as a "cationizing" reagent (cocatalyst, cf. Scheme 1). The precatalyst mixture was aged for 30 min at ambient temperature prior to addition of isoprene. A catalyst-to-monomer ratio of 1:1000 was realized in all of the experiments which were carried out at 40 °C for 24 h in hexane solutions. Conversions, stereospecificities, and molecular weights are summarized in Table 5.

To elucidate the influence of the metal centers on the catalytic activity, the alkylated lanthanide carboxylates **12a**−**e** were used as precatalyst components at constant n_{Cl}:n_{Ln} ratios of 1:1 (runs 1, 3, 7, 10, and 11). The yttrium (**12a**) and lutetium derivatives (**12e**) were completely inactive, whereas polymer yields increased for the larger metal centers in the order La < Gd < Nd (12, 24, 77%). This behavior is in agreement with previously published activity orders.[18a,49]

Scheme 7. Carboxylate−Alkyl Interchange: A Mechanistic Scenario of the Formation of Differently Alkylated Lanthanide Carboxylate Complexes[a]

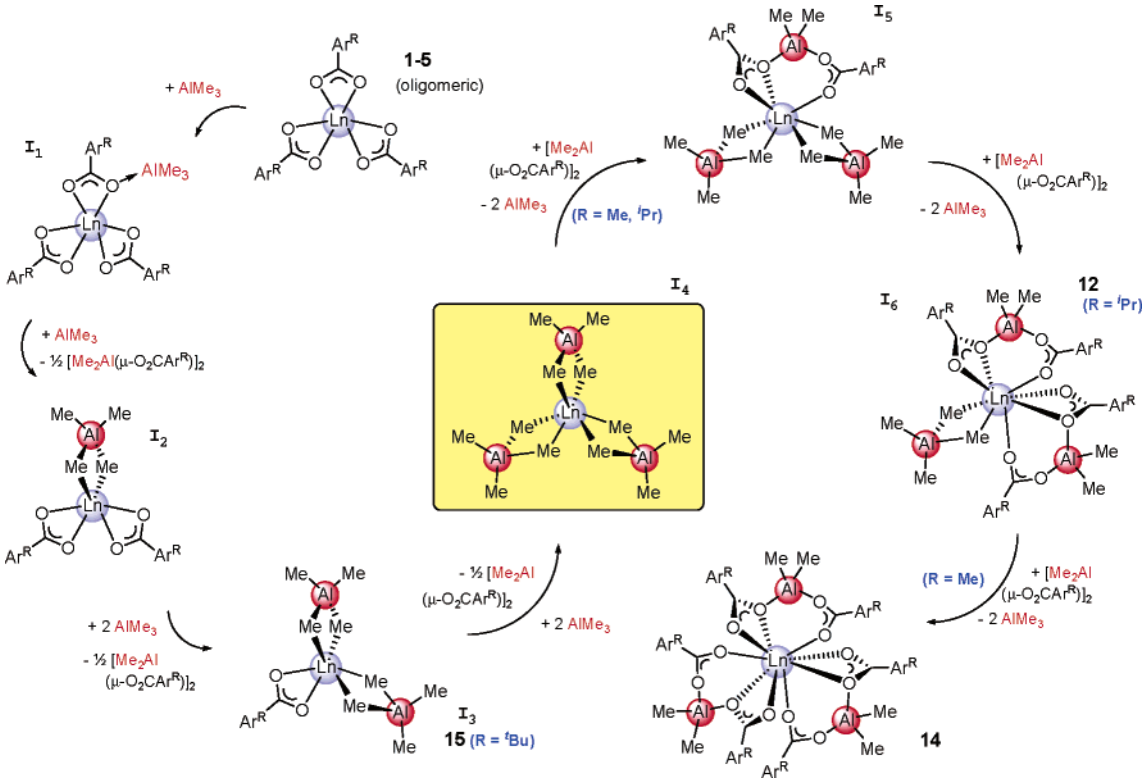

[a] Except for I_1, I_2, and I_5 all Ln complexes were completely characterized; $Ar^R = C_6H_2R'_3$-2,4,6 or $C_6H_3R'_2$-2,6.

Table 5. Effect of Metal Size and Degree of Alkylation (Steric Bulk of Benzoate Ligands) on Ln-Based Polymerization of Isoprene after 24 h

run[a]	precat.	n_{Cl}:n_{Ln}[b]	conv/%	*cis*-1,4[c]/%	M_n[d] (×10³)	M_w[d] (×10³)	PDI[d]
1	**12a**	1:1	0				
2	**12b**	0:1	0				
3	**12b**	1:1	12	95.1	137	558	4.08
4	**12b**	2:1	70	98.1	180	816	4.52
5	**12b**	3:1	21	> 99	100	452	4.52
6	**12c**	0:1	0				
7	**12c**	1:1	77	93.5	165	575	3.48
8	**12c**	2:1	>99	98.6	271	621	2.29
9	**12c**	3:1	98	>99	194	410	2.11
10	**12d**	1:1	24	92.0	112	589	5.27
11	**12e**	1:1	0				
12	**13b**	1:1	97	94.3	78	290	3.73
13	**13b**	2:1	>99	96.6	91	454	4.98
14	**13b**	3:1	60	>99	66	217	3.27
15	**13c**	1:1	97	90.7	94	297	3.16
16	**13c**	2:1	>99	95.6	92	266	2.88
17	**13c**	3:1	>99	98.7	78	229	2.94
18	**15b**	1:1	83	97.5	125	593	4.76
19	**15b**	2:1	>99	>99	175	564	3.23
20	**15b**	3:1	86	>99	57	307	5.37
21	**15c**	1:1	>99	98.7	277	787	2.84
22	**15c**	2:1	>99	>99	250	705	2.82
23	**15c**	3:1	>99	>99	165	462	2.79

[a] Polymerization procedure: 0.02 mmol of precatalyst, 8 mL of hexane, 0.02−0.06 mmol of Et_2AlCl (1−3 equiv), 20 mmol of isoprene; 24 h, 40 °C. [b] Catalyst preformation 30 min at room temperature. [c] Measured by means of ^{13}C NMR spectroscopy in $CDCl_3$. [d] Determined by means of size exclusion chromatography (SEC) against polystyrene standards.

The tetraethylaluminate derivatives **13b** (Ln = La) and **13c** (Ln = Nd) displayed higher activity and also gave almost quantitative conversions for the lanthanum derivative (runs 12 and 15). Therefore, a distinct metal effect was not observed for n_{Cl}:n_{Ln} ratios of 1:1 and 2:1 within the reaction time of 24 h. This increased catalytic activity can be rationalized on the enhanced solubility of the tetraethylaluminate versus the tetramethylaluminate Ln components (see below). In general, the stereospecificities and activities could be improved by increasing the amount of the halide-transferring cocatalyst. For the tetramethylaluminate derivatives **12b** (Ln = La) and **12c** (Ln = Nd) a larger n_{Cl}:n_{Ln} ratio (2:1, 3:1; runs 4, 5, 8, and 9) increased both the *cis*-1,4-polymerization and monomer conversion. This is in agreement with literature reports on lanthanide carboxylate-based catalysts showing the highest conversions in diene polymerization at n_{Cl}:n_{Ln} ratios of ∼2.[50] After 24 h **12c** quantitatively polymerized isoprene under these conditions (run 8), whereas polymer yields for the lanthanum derivative **12b** increased from 12 to 70% (runs 3 versus 4). At n_{Cl}:n_{Ln} ratios ≥ 3 polymer yields decreased again, due to the likely formation of higher halogenated and hence more insoluble lanthanide species. However, for complexes **12b** and **12c** maximum *cis*-1,4-contents (>99%; only *cis*-signals in the ^{13}C NMR) were observed only at n_{Cl}:n_{Ln} ratios of 3 and larger (runs 5 and 9).

The molecular weights of the isolated polymers show relatively similar values for the tetramethylaluminate derivatives **12b−d**; however, the molecular weight distributions (MWD) strongly depend on the metal center. The lowest polydispersities of 2.29 and 2.11 were realized for the most active mono(tetramethylaluminate) neodymium complex **12c** at n_{Cl}:n_{Ln} = 2 and 3, respectively (runs 8 and 9). All of the GPC elugrams show polymodal mass distributions indicating two or three catalytically active species.

(49) (a) Shen, Z. *Inorg. Chim. Acta* **1987**, *140*, 7. (b) Wang, S.; Li, Z.; Wang, F. *Polym. Commun.* **1984**, 425.

(50) (a) Witte, J. *Angew. Macromol. Chem.* **1981**, *94*, 119. (b) Pross, A.; Marquardt, P.; Reichert, K. H.; Nentwig, W.; Knauf, T. *Angew. Macromol. Chem.* **1993**, *211*, 89. (c) Friebe, L.; Nuyken, O.; Windisch, H.; Obrecht, W. *Macromol. Chem. Phys.* **2002**, *203*, 1055.

Scheme 8. Proposed Mechanistic Scenario of the Formation of the Active Species for Mono(tetramethylaluminate) Complexes 12

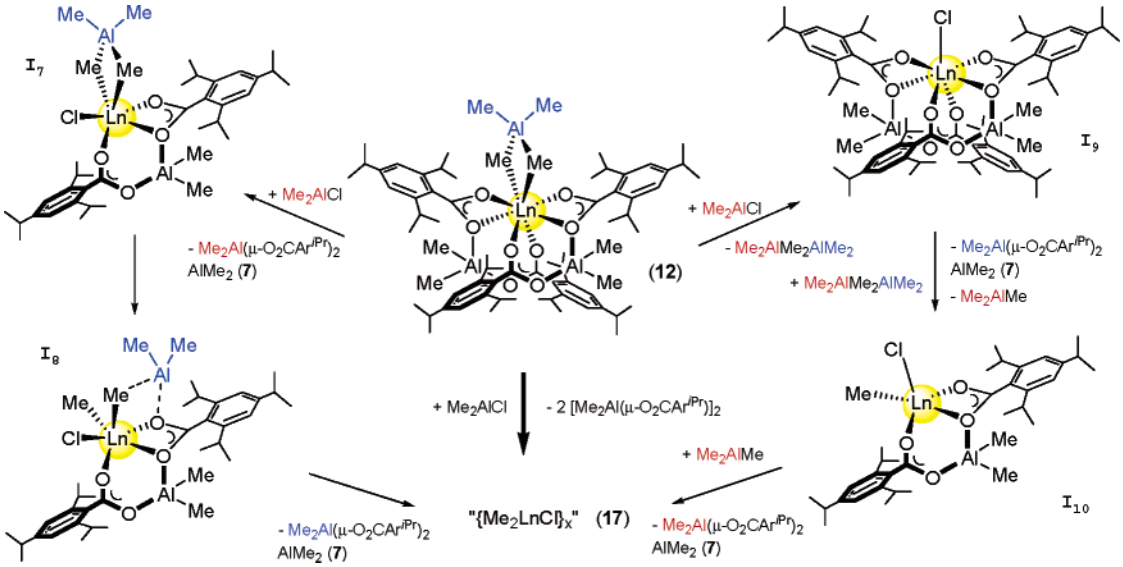

Mono(carboxylate) bis(tetramethylaluminates) **15b** and **15c** displayed an even higher catalytic activity, producing polyisoprene in high to quantitative yields within 24 h (runs 18−23). Compared with the mono(tetraalkylaluminate) complexes **12** and **13**, *cis*-contents of the polymers were higher (>97.5%), even in the presence of only 1 equiv of Et_2AlCl. On the other hand, molecular weights and molecular weight distributions were similar to those obtained via the mono(tetramethylaluminate) complexes, showing broader distributions for the less active lanthanum derivative(s).

Reactivity of 12a and 12b with R_2AlCl. In order get a deeper insight into the structure−reactivity relationship of the formation of the catalytically active binary system, we examined the interaction of the "cationizing" chloride-donating reagent with the alkylated rare-earth metal centers of complexes **12** (cf. Scheme 1). Accordingly, complexes **12a** and **12b** were reacted with equimolar amounts of Me_2AlCl in hexane solutions. Immediately after the addition of the Al cocatalyst a white precipitate formed, which was separated after 2 h via centrifugation. The supernatant hexane solution was dried in vacuo and investigated by NMR spectroscopy. Surprisingly, only one soluble product formed, which could be identified as the dimeric dimethylaluminum-bridged carboxylate **7**. Quantitative yields of **7** indicated that both chelating bis(carboxylate) ligands in **12a** and **12b** were cleaved by the addition of only 1 equiv of Me_2AlCl. Although the elemental analyses of the insoluble lanthanide-containing products were not satisfactory, the amount of insoluble products points at the formation of polymeric/ionic "$\{Me_2LnCl\}_x$" (**17**) as a possible polymerization-inititating species. A mechanistic scenario for this activation sequence is presented in Scheme 8.

We suggest two possible reaction pathways for the interaction of Me_2AlCl with complexes **12**. As shown on the left-hand side, addition of 1 equiv of the alkylaluminum reagent causes an Al → Ln chloride transfer with a simultaneous cleavage of one of the $AlMe_2$-bridged bis(carboxylate) ligands, forming intermediate $\mathbf{I_7}$. Then, the Ln-bonded tetramethylaluminate unit undergoes a reorientation by breaking one of the Al−C(Me) bonds and forming an Al−O interaction, which is known from Ln−Al heterobimetallic alkoxide[23,24,51] and aryloxide[26,27] chemistry. From intermediate $\mathbf{I_8}$, featuring a terminal methyl group, the second biscarboxylate ligand dissociates, finally forming highly reactive polymeric "$\{Me_2LnCl\}_x$". On the other hand, initial cleavage of the tetramethylaluminate unit in **12** has to be taken into consideration. Correspondingly, the reaction path on the right-hand side involves the formation of a terminal chloride ligand in intermediate $\mathbf{I_9}$ via addition of Me_2AlCl. Subsequently, released Al_2Me_6 causes the cleavage of both of the bis(carboxylate) ligands in a two-step reaction.

Although none of the intermediates $\mathbf{I_7}$−$\mathbf{I_{10}}$ could be isolated, several additional experiments support the reaction sequence presented in Scheme 8. According to a "AlR_3 cross experiment" (eq 11), addition of 1 equiv of Et_2AlCl instead of Me_2AlCl to mono(tetramethylaluminate) complex **12b** produced a mixture of several hexane-soluble species, as indicated by proton NMR spectroscopy. Although crystallization failed due to similar solubilities, the dimethylaluminum-bridged bis(carboxylate) **7** was formed as one of the products, as expected from the mechanistic scenario. On the other hand, addition of 1 equiv of Et_2AlCl to the mono(tetraethylaluminate) complex **13b** produced **11** exclusively, as indicated by ^1H NMR spectroscopy (eq 12); no mixed-alkylated species were generated.

$$\mathbf{12b} + Et_2AlCl \rightarrow [Me_2Al(\mu\text{-}O_2CAr^{iPr})]_2\ (\mathbf{7}) + \text{other products} \quad (11)$$

$$\mathbf{13b} + Et_2AlCl \rightarrow [Et_2Al(\mu\text{-}O_2CAr^{iPr})]_2\ (\mathbf{11}) + \text{other products} \quad (12)$$

Furthermore, given the thermal stability of "$LnMe_3$",[52] one can also speculate about a ligand disproportionation reaction of "monocationic" "$\{Me_2LnCl\}_x$" into "$\{LnMe_3\}_x$" and "$\{LnCl_3\}_x$". At n_{Cl}:n_{Ln} ratios ≥ 2, "dicationic" "$\{MeLnCl_2\}_x$" seems to be a chemically sound and realistic activation product.[53]

(51) Evans, W. J.; Boyle, T. J.; Ziller, J. W. *J. Organomet. Chem.* **1993**, *462*, 141.
(52) Dietrich, H. M.; Raudaschl-Sieber, G.; Anwander, R. *Angew. Chem., Int. Ed.* **2005**, *44*, 5303.
(53) (a) Maiwald, S.; Weissenborn, H.; Windisch, H.; Sommer, C.; Müller, G.; Taube, R. *Macromol. Chem. Phys.* **1997**, *198*, 3305. (b) Maiwald, S.; Taube, R.; Hemling, H.; Schumann, H. *J. Organomet. Chem.* **1998**, *552*, 195. (c) Ward, B. D.; Bellemin-Laponnaz, S.; Gade, L. H. *Angew. Chem., Int. Ed.* **2005**, *44*, 1668. (d) Arndt, S.; Beckerle, K.; Zeimentz, P. M.; Spaniol, T. P.; Okuda, J. *Angew. Chem., Int. Ed.* **2005**, *44*, 7473.

Scheme 9. Allyl Insertion Mechanism of 1,3-Diene Polymerization Taking into Account Organoaluminum-Mediated Chain Transfer

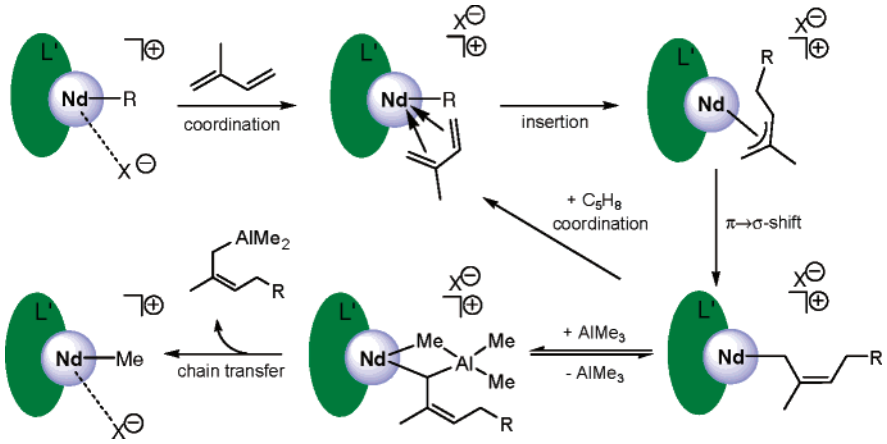

However, given the ready availability of organoaluminum reagents in the reaction mixtures, equilibria reactions involving species "$\{Me_2LnCl\}_x(AlR_3)_y$" and "$\{MeLnCl_2\}_x(AlR_3)_z$" have to be taken into account as well.

Conclusions

The interaction of tailor-made rare-earth metal benzoate complexes $\{Ln(O_2CAr^R)_3\}_x$ with homoleptic organoaluminum reagents AlR'_3 (R′ = Me, Et) reveals an unprecedented alkylation and carboxylate ligand rearrangement sequence depending on the steric bulk of the carboxylate substituents R. Variable-temperature NMR studies and X-ray crystallographic analyses give precise insight into the metal-size-dependent dynamic behavior of the tetraalkylaluminate ligand and the coordination features of heteroleptic mono- and bis(tetraalkylaluminate) complexes $[Me_2Al(O_2CC_6H_2iPr_3\text{-}2,4,6)_2]_2Ln[(\mu\text{-}Me)_2AlMe_2]$ and $\{Ln(O_2CC_6H_2tBu_3\text{-}2,4,6)[(\mu\text{-}Me)_2AlMe_2]_2\}_2$, respectively. This intrinsic (ligand-dependent) alkylation amenability certainly hampers a direct comparison with industrially applied versatate- and naphthenoate-coordinated neodymium centers; however, the formation of tetraalkylaluminate moieties seems to be a preferred reaction pathway. The accessibility of the various alkylated carboxylate complexes via reaction of homoleptic $Ln(AlMe_4)_3$ with benzoic acids or alkylation byproducts $[R_2AlO_2CAr^R]$ suggests a crucial role of the tris(tetraalkylaluminate) Ln complexes. The enhanced thermodynamic and kinetic lability of tetraalkylaluminate ligands bonded to large rare-earth metal centers and the existence of extensive Al-to-Ln and Ln-to-Al ligand transfer sequences, including $[O_2CAr^{iPr}] \rightarrow [AlMe_4]$ and $[AlMe_3] \rightarrow [Me_2Al(O_2CAr^{iPr})_2]$ transformations, underline the ease of polymer chain transfer via Ln−Al heterobimetallic complexes in Ziegler-type catalysts. This is realized in a modified allyl insertion mechanism of isoprene polymerization as shown in Scheme 9.

A comprehensive study of isoprene polymerization revealed that the alkylated Ln−Al heterobimetallic carboxylate complexes are highly efficient precatalyst components in binary Ziegler-type catalysts. After activation with Et_2AlCl, the catalyst systems confirm classic features of rare-earth metal carboxylate-based catalysts such as high *cis*-1,4 polymerization (>99%), neodymium as the most active metal center ("neodymium effect"), and a favorable n_{Cl}:n_{Ln} ratio of ∼2. In addition, the polymerization efficiency depends on the degree of alkylation ("$Ln(AlMe_4)_3$" > "$Ln(AlMe_4)_2$" > "$Ln(AlMe_4)$"). Finally, the broad molecular weight distributions, which usually result from solution polymerizations with such multicomponent Ziegler-type catalysts, are consistent with pronounced Ln-to-Al polymer chain transfer.

Experimental Section

General Considerations. All operations were performed with rigorous exclusion of air and water, using high-vacuum and glovebox techniques (MBraun MB150B-G-II; <1 ppm O_2, <1 ppm H_2O). Solvents were predried and distilled from Na/K alloy (benzophenone ketyl) under argon. Deuterated solvents were obtained from Merck. C_6D_6 and THF-d_8 were degassed and dried over Na/K alloy; DMSO-d_6 was used without further purification. 2,4,6-Trimethylbenzoic acid was obtained from Aldrich, and 2,4,6-triisopropylbenzoic acid from ABCR; both were used without further purification. 2,4,6-Tri-*tert*-butylbenzoic acid,[54] 2,6-diphenylbenzoic acid,[55] and 2,6-dimesitylbenzoic acid[55] were synthesized according to literature procedures. The lanthanide silylamide precursors $Ln[N(SiMe_3)_2]_3$ (Ln = Y, La, Nd, Gd, Lu) were synthesized according to the literature.[31] Trimethylaluminum, triethylaluminum, dimethylaluminum chloride, and diethylaluminum chloride were purchased from Aldrich and used as received. **CAUTION:** Alkylaluminum reagents react violently with moisture. Isoprene was dried over molecular sieves (3 Å) and distilled prior to use.

NMR spectra were recorded either on a JEOL-GX-400 (FT, 399.78 MHz ^1H; 100.5 MHz ^{13}C) or on a JEOL JNM-GX-270 (FT, 270.16 MHz ^1H; 67.93 MHz ^{13}C) spectrometer. ^1H and ^{13}C shifts are referenced to internal solvent resonances and reported relative to TMS. IR spectra were recorded on a Perkin-Elmer 1650-FTIR spectrometer as Nujol mulls or KBr pellets. Elemental analyses were performed in the microanalytical laboratory of TUM.

General Procedure for the Synthesis of Rare-Earth Metal Carboxylates. To a solution of $Ln[N(SiMe_3)_2]_3$ in THF was slowly added a solution of 3 equiv of the chosen carboxylic acid in THF at −45 °C, and the resulting mixture was stirred at ambient temperature overnight. Then, the solvent and the volatile byproducts were removed in vacuo. The remaining solid was washed several times with hexane. After drying for several hours the powdery products were isolated in high yields.

$\{Y(O_2CC_6H_2Me_3\text{-}2,4,6)_3\}_n$ (1a). Following the procedure described above, $Y[N(SiMe_3)_2]_3$ (0.855 g, 1.50 mmol) and HO_2CAr^{Me} (0.739 g, 4.50 mmol) yielded **1a** as a colorless, THF-insoluble solid (0.850 g, 1.47 mmol, 98%). IR (KBr): 3000 s, 2958 s, 2922 s,

(54) Betts, E. E.; Barclay, L. R. C. *Can. J. Chem.* **1955**, *33*, 1768.
(55) (a) Du, C.-J. F.; Hart, H.; Ng, K.-K. D. *J. Org. Chem.* **1986**, *51*, 3162. (b) Saednya, A.; Hart, H. *Synthesis* **1996**, 1455. (c) Waller, S. C.; Mash, E. A. *Org. Prep. Proc. Int.* **1997**, *29*, 679. (d) Lüning, U.; Wangnick, C.; Peters, K.; von Schnering, H. G. *Chem. Ber.* **1991**, *124*, 397.

2854 m, 2731 w, 1718 w, 1607 s, 1522 s, 1427 s, 1294 m, 1252 m, 1182 s, 1116 s, 1040 m, 844 s, 825 m, 795 m, 747 m, 608 s, 599 s, 568 w cm^{-1}. ^{1}H NMR (DMSO-d_6): δ 6.73 (s, 6 H, Ar-*H*), 2.25 (s, 18 H, o-*Me*), 2.18 (s, 9 H, p-*Me*). ^{13}C{^{1}H} NMR (DMSO-d_6): δ 180.5 (*C*OO), 137.0, 135.7, 133.4, 127.4, 20.6 (p-*Me*), 19.7 (o-*Me*). Anal. Calcd for $C_{30}H_{33}O_6Y$: C, 62.29; H, 5.75. Found: C, 62.38; H, 5.80.

{La(O$_2$CC$_6$H$_2$Me$_3$-2,4,6)$_3$}$_n$ (1b). Following the procedure described above, La[N(SiMe$_3$)$_2$]$_3$ (0.931 g, 1.50 mmol) and HO$_2$CAr^{Me} (0.739 g, 4.50 mmol) yielded **1b** as a colorless, THF-insoluble solid (0.899 g, 1.43 mmol, 95%). IR (Nujol): 1610 m, 1574 w, 1517 s, 1307 w, 1180 m, 1112 w, 1031 w, 846 w, 834 m, 801 w, 608 m cm^{-1}. ^{1}H NMR (DMSO-d_6): δ 6.73 (s, 6 H, Ar-*H*), 2.27 (s, 18 H, o-*Me*), 2.18 (s, 9 H, p-*Me*). ^{13}C{^{1}H} NMR (DMSO-d_6): δ 181.2 (*C*OO), 137.9, 135.2, 133.2, 127.3, 20.5 (p-*Me*), 19.7 (o-*Me*). Anal. Calcd for $C_{30}H_{33}LaO_6$: C, 57.33; H, 5.29. Found: C, 57.91; H, 5.41.

{Nd(O$_2$CC$_6$H$_2$Me$_3$-2,4,6)$_3$}$_n$ (1c). Following the procedure described above, Nd[N(SiMe$_3$)$_2$]$_3$ (0.938 g, 1.50 mmol) and HO$_2$CAr^{Me} (0.739 g, 4.50 mmol) yielded **1c** as a light blue, THF-insoluble solid (0.878 g, 1.39 mmol, 92%). IR (Nujol): 3000 s 2959 s, 2922 s, 2856 m, 1718 w, 1611 s, 1518 s, br, 1250 m, 1181 s, 1113 s, 1035 m, 933 m, 889 m, 832 s, 802 m, 728 m, 602 s, 566 m cm^{-1}. Anal. Calcd for $C_{30}H_{33}NdO_6$: C, 56.85; H, 5.25. Found: C, 56.58; H, 5.14.

{Y(O$_2$CC$_6$H$_2$*i*Pr$_3$-2,4,6)$_3$}$_n$ (2a). Following the procedure described above, Y[N(SiMe$_3$)$_2$]$_3$ (1.140 g, 2.00 mmol) and HO$_2$CAr^{iPr} (1.490 g, 6.00 mmol) yielded **2a** (1.576 g, 95%) as a colorless solid. IR (KBr): 2964 s, 2926 s, 2869 s, 1683 m, 1607 s, 1520 s, 1461 s, 1416 s, 1362 s, 1318 m, 1157 m, 1109 m, 1070 m, 940 m, 874 s, 791 m, 617 m cm^{-1}. ^{1}H NMR (THF-d_8): δ 7.00 (s, 6 H, Ar-*H*), 3.29 (septet, $^3J_{HH}$ = 6.7 Hz, 6 H, o-C*H*Me$_2$), 2.87 (septet, $^3J_{HH}$ = 6.7 Hz, 3 H, p-C*H*Me$_2$), 1.23 (d, $^3J_{HH}$ = 6.7 Hz, 54 H, o/p-CH*Me*$_2$). ^{13}C{^{1}H} NMR (THF-d_8): δ 187.7 (*C*OO), 149.3, 145.0, 136.0, 120.9, 35.4 (p-*C*HMe$_2$), 31.8 (o-*C*HMe$_2$), 24.8 (o-CH*Me*$_2$), 24.4 (p-CH*Me*$_2$). Anal. Calcd for $C_{48}H_{69}O_6Y$: C, 69.38; H, 8.37. Found: C, 69.41; H, 8.54.

{La(O$_2$CC$_6$H$_2$*i*Pr$_3$-2,4,6)$_3$}$_n$ (2b). Following the procedure described above, La[N(SiMe$_3$)$_2$]$_3$ (1.240 g, 2.00 mmol) and HO$_2$CAr^{iPr} (1.490 g, 6.00 mmol) yielded **2b** (1.695 g, 96%) as a colorless solid. IR (KBr): 2954 s, 2924 s, 2868 s, 1671 m, 1608 s, 1518 s, 1461 s, 1410 s, 1361 s, 1317 m, 1156 m, 1108 m, 1070 m, 940 m, 874 s, 790 m, 616 m cm^{-1}. ^{1}H NMR (THF-d_8): δ 6.93 (s, 6 H, Ar-*H*), 3.43 (septet, $^3J_{HH}$ = 7.0 Hz, 6 H, o-C*H*Me$_2$), 2.83 (septet, $^3J_{HH}$ = 7.0 Hz, 3 H, p-C*H*Me$_2$), 1.22 (d, $^3J_{HH}$ = 7.0 Hz, 18 H, p-CH*Me*$_2$), 1.17 (d, $^3J_{HH}$ = 7.0 Hz, 36 H, o-CH*Me*$_2$). ^{13}C{^{1}H} NMR (THF-d_8): δ 186.1 (*C*OO), 148.4, 145.2, 137.4, 120.8, 35.4 (p-*C*HMe$_2$), 31.4 (o-*C*HMe$_2$), 25.0 o-CH*Me*$_2$), 24.5 (p-CH*Me*$_2$). Anal. Calcd for $C_{48}H_{69}LaO_6$: C, 65.44; H, 7.89. Found: C, 64.97; H, 8.16.

{Nd(O$_2$CC$_6$H$_2$*i*Pr$_3$-2,4,6)$_3$}$_n$ (2c). Following the procedure described above, Nd[N(SiMe$_3$)$_2$]$_3$ (0.625 g, 1.00 mmol) and HO$_2$CAr^{iPr} (0.745 g, 3.00 mmol) yielded **2c** (0.843 g, 95%) as a light blue solid. IR (KBr): 2965 s, 2925 s, 2869 s, 1674 m, 1608 s, 1516 s, 1459 s, 1408 s, 1361 s, 1318 m, 1156 m, 1109 m, 1070 m, 940 m, 874 s, 791 m, 616 m cm^{-1}. Anal. Calcd for $C_{48}H_{69}NdO_6$: C, 65.05; H, 7.85. Found: C, 64.81; H, 7.73.

{Gd(O$_2$CC$_6$H$_2$*i*Pr$_3$-2,4,6)$_3$}$_n$ (2d). Following the procedure described above, Gd[N(SiMe$_3$)$_2$]$_3$ (0.638 g, 1.00 mmol) and HO$_2$CAr^{iPr} (0.745 g, 3.00 mmol) yielded **2d** (0.841 g, 93%) as a white solid. IR (KBr): 2957 s, 2924 s, 2869 s, 1674 m, 1607 s, 1513 s, br, 1460 s, 1416 s, br, 1382 s, 1361 s, 1318 m, 1243 w, 1156 m, 1109 m, 1070 w, 940 w, 874 s, 791 m, 618 m cm^{-1}. Anal. Calcd for $C_{48}H_{69}GdO_6$: C, 64.11; H, 7.73. Found: C, 63.72; H, 7.79.

{Lu(O$_2$CC$_6$H$_2$*i*Pr$_3$-2,4,6)$_3$}$_n$ (2e). Following the procedure described above, Lu[N(SiMe$_3$)$_2$]$_3$ (0.656 g, 1.00 mmol) and HO$_2$CAr^{iPr} (0.745 g, 3.00 mmol) yielded **2e** (0.891 g, 97%) as a colorless solid. IR (KBr): 2960 s, 2923 s, 2868 s, 1684 m, 1608 s, 1527 s, 1460 s, 1424 s, 1381 m, 1362 s, 1318 m, 1158 m, 1110 m, 1070 m, 940 m, 874 s, 792 m, 616 m cm^{-1}. ^{1}H NMR (DMSO-d_6): δ 6.95 (s, 6 H, Ar-*H*), 3.27 (septet, $^3J_{HH}$ = 6.6 Hz, 6 H, o-C*H*Me$_2$), 2.83 (septet, $^3J_{HH}$ = 6.6 Hz, 3 H, p-C*H*Me$_2$), 1.18 (d, $^3J_{HH}$ = 6.6 Hz, 18 H, p-CH*Me*$_2$), 1.15 (d, $^3J_{HH}$ = 6.6 Hz, 36 H, o-CH*Me*$_2$). ^{13}C{^{1}H} NMR (DMSO-d_6): δ 183.3 (*C*OO), 147.4, 143.4, 135.9, 119.8, 33.5 (p-*C*HMe$_2$), 29.9 (o-*C*HMe$_2$), 24.2 o-CH*Me*$_2$), 23.9 (p-CH*Me*$_2$). Anal. Calcd for $C_{48}H_{72}LuO_6$: C, 62.87; H, 7.58. Found: C, 62.25; H, 7.33.

{Y(O$_2$CC$_6$H$_2$*t*Bu$_3$-2,4,6)$_3$(THF)}$_n$ (3a). Following the procedure described above, Y[N(SiMe$_3$)$_2$]$_3$ (0.855 g, 1.50 mmol) and HO$_2$CAr^{tBu} (1.307 g, 4.50 mmol) yielded **3a** (1.348 g, 87%) as a colorless solid. IR (KBr): 2965 s, 2912 s, 2868 s, 1700 m, 1604 s, 1552 s, 1527 s, 1495 s, 1457 s, 1394 s, 1356 s, 1267 m, 1244 m, 1217 m, 1091 w, 1010 w, 912 w, 878 m, 846 m, 807 m, 770 m, 674 w, 650 w, 603 w cm^{-1}. ^{1}H NMR (THF-d_8): δ 7.43 (s, 6 H, Ar-*H*), 3.63 (m, 4 H, THF), 1.78 (m, 4 H, THF), 1.52 (s, 54 H, o-C*Me*$_3$), 1.33 (s, 27 H, p-C*Me*$_3$). ^{13}C{^{1}H} NMR (THF-d_8): δ 193.3 (*C*OO), 149.9, 147.0, 133.5, 122.5, 68.2 (THF), 37.9 (o-*C*Me$_3$), 35.6 (p-*C*Me$_3$), 33.3 (o-C*Me*$_3$), 31.7 (p-C*Me*$_3$), 25.4 (THF). Anal. Calcd for $C_{61}H_{95}O_7Y$: C, 71.18; H, 9.30. Found: C, 71.22; H, 9.04.

{La(O$_2$CC$_6$H$_2$*t*Bu$_3$-2,4,6)$_3$(THF)}$_n$ (3b). Following the procedure described above, La[N(SiMe$_3$)$_2$]$_3$ (0.868 g, 1.40 mmol) and HO$_2$CAr^{tBu} (1.220 g, 4.20 mmol) yielded **3b** (1.252 g, 83%) as a colorless solid. IR (KBr): 2972 s, br, 2900 s, 2861 s, 1697 s, 1603 s, 1535 s, br, 1461 s, 1399 s, 1363 s, 1267 s, 1244 s, 1218 s, 1174 m, 1136 w, 1093 m, 1027 w, 984 m, 911 m, 876 s, 842 m, 807 s, 782 m, 652 m, 590 s, 486 m cm^{-1}. ^{1}H NMR (DMSO-d_6): δ 7.21 (s, 6 H, Ar-*H*), 3.59 (m, 4 H, THF), 1.75 (m, 4 H, THF), 1.45 (s, 54 H, o-C*Me*$_3$), 1.24 (s, 27 H, p-C*Me*$_3$). ^{1}H NMR (THF-d_8): δ 7.36 (s, 6 H, Ar-*H*), 1.47 (s, 54 H, o-C*Me*$_3$), 1.31 (s, 27 H, p-C*Me*$_3$). ^{13}C{^{1}H} NMR (THF-d_8): δ 188.5 (*C*OO), 148.3, 146.1, 136.2, 122.1, 37.7 (o-*C*Me$_3$), 35.5 (p-*C*Me$_3$), 33.2 (br, o-C*Me*$_3$), 31.7 (p-C*Me*$_3$). Anal. Calcd for $C_{61}H_{95}LaO_7$: C, 67.88; H, 8.87. Found: C, 67.01; H, 9.40.

{Y(O$_2$CC$_6$H$_3$Ph$_2$-2,6)$_3$(THF)}$_n$ (4a). Following the procedure described above, Y[N(SiMe$_3$)$_2$]$_3$ (0.570 g, 1.00 mmol) and HO$_2$CAr^{Ph} (0.823 g, 3.00 mmol) yielded **4a** (0.832 g, 85%) as a colorless solid. IR (Nujol): 1583 w, 1571 w, 1535 m, 1523 m, 1494 w, 1438 s, 1304 w, 1283 w, 1182 w, 1148 w, 1072 w, 1028 m, 916 w, 880 w, 856 m, 754 s, 701 s, 616 w, 534 m, 427 w cm^{-1}. ^{1}H NMR (THF-d_8): δ 7.43 (d, $^3J_{HH}$ = 7.0 Hz, 12 H, o-*Ph*), 7.37 (t, $^3J_{HH}$ = 7.7 Hz, 3 H, p-Ar-*H*), 7.22 (d, $^3J_{HH}$ = 7.7 Hz, 6 H, m-Ar-*H*), 7.17−7.08 (m, 18 H, m-*Ph*, p-*Ph*), 3.63 (m, 4 H, THF), 1.79 (m, 4 H, THF). ^{13}C{^{1}H} NMR (THF-d_8): δ 181.9 (*C*OO), 143.0, 140.9, 137.6, 130.1, 128.5, 128.0, 126.9, 68.1 (THF), 26.3 (THF). Anal. Calcd for $C_{61}H_{47}O_7Y$: C, 74.69; H, 4.83. Found: C, 72.60; H, 5.71.

{La(O$_2$CC$_6$H$_3$Ph$_2$-2,6)$_3$(THF)}$_n$ (4b). Following the procedure described above, La[N(SiMe$_3$)$_2$]$_3$ (0.873 g, 1.35 mmol) and HO$_2$CAr^{Ph} (1.111 g, 4.05 mmol) yielded **4b** (1.272 g, 91%) as a colorless solid. IR (Nujol): 1581 w, 1570 w, 1512 s, br, 1494 s, 1443 s, 1308 m, 1171 w, 1155 w, 1076 w, 1028 w, 973 w, 919 w, 868 m, 847 s, 766 s, 755 s, 700 s, 648 m, 614 m, 521 m, 428 m cm^{-1}. ^{1}H NMR (THF-d_8): δ 7.44 (d, $^3J_{HH}$ = 7.3 Hz, 12 H, o-*Ph*), 7.34 (t, $^3J_{HH}$ = 7.7 Hz, 3 H, p-Ar-*H*), 7.22−7.17 (m, 18 H, m-Ar-*H*, m-*Ph*), 7.06 (t, $^3J_{HH}$ = 7.4 Hz, 6 H, p-*Ph*), 3.63 (m, 4 H, THF), 1.79 (m, 4 H, THF). ^{13}C{^{1}H} NMR (THF-d_8): δ 182.7 (*C*OO), 143.3, 141.1, 138.6, 129.9, 128.7, 127.8, 126.6, 68.1 (THF), 26.3 (THF). Anal. Calcd for $C_{61}H_{47}LaO_7$: C, 71.07; H, 4.60. Found: C, 70.19; H, 5.09.

{Y(O$_2$CC$_6$H$_3$Mes$_2$-2,6)$_3$(THF)}$_n$ (5a). Following the procedure described above, Y[N(SiMe$_3$)$_2$]$_3$ (0.570 g, 1.00 mmol) and HO$_2$CAr^{Mes} (1.075 g, 3.00 mmol) yielded **5a** (1.111 g, 90%) as a colorless solid. ^{1}H NMR (DMSO-d_6): δ 7.39 (s, br, 3 H, p-Ar-*H*), 6.83 (s, br, 6 H, m-Ar-*H*), 6.76 (s, 12 H, m-*Ph*), 3.59 (m, 4 H, THF), 2.22 (s, 18 H, p-*Me*), 1.91 (s, 36 H, o-*Me*), 1.75 (m, 4 H,

THF). $^{13}C\{^1H\}$ NMR (THF-d_8): δ 179.8 (*C*OO), 139.5, 139.1, 136.1, 134.9, 134.2, 128.4, 127.4, 126.8, 67.0 (THF), 25.1 (THF), 20.6 (o-*Me*), 20.5 (p-*Me*). Anal. Calcd for $C_{79}H_{83}O_7Y$: C, 76.93; H, 6.78. Found: C, 76.54; H, 6.63.

$\{La(O_2CC_6H_3Mes_2\text{-}2,6)_3(THF)\}_n$ (5b). Following the procedure described above, $La[N(SiMe_3)_2]_3$ (0.701 g, 1.13 mmol) and HO_2CAr^{Mes} (0.930 g, 3.39 mmol) yielded **5b** (1.343 g, 93%) as a colorless solid. IR (KBr): 2953 s, 2916 s, 2854 m, 1741 w, 1610 m, 1579 s, 1524 s, br, 1484 s, 1453 s, 1437 s, 1384 s, 1145 w, 1066 w, 1031 m, 850 s, 771 m, 710 m, 589 m, 575 w, 452 m cm^{-1}. ^1H NMR (DMSO-d_6): δ 7.25 (s, br, 3 H, p-Ar-*H*), 6.8−6.7 (m, 18 H, m-Ar-*H*, m-*Ph*), 3.59 (m, 4 H, THF), 2.21 (s, 18 H, p-*Me*), 1.94 (s, 36 H, o-*Me*), 1.75 (m, 4 H, THF). $^{13}C\{^1H\}$ NMR (DMSO-d_6): δ 179.9 (*C*OO), 139.4, 138.6, 137.8, 135.5, 135.4, 134.2, 127.7, 127.1, 66.9 (THF), 25.0 (THF), 20.6 (o-*Me*), 20.5 (p-*Me*). Anal. Calcd for $C_{79}H_{83}LaO_7$: C, 73.93; H, 6.52. Found: C, 73.42; H, 6.39.

General Procedures for the Synthesis and Isolation of Alkylated Rare-Earth Metal Carboxylates. Procedure A. In a glovebox, 6 equiv of TMA were added to the homoleptic carboxylate complexes suspended in hexane. After stirring the suspension overnight at ambient temperature, the reaction mixture was centrifuged, and the insoluble product was washed several times with hexane. After drying for several hours the heteroleptic aluminate complexes were obtained as colorless solids in moderate yields.

Procedure B. In a glovebox, 3 or 4 equiv of TMA (or TEA) were added to the precursor carboxylate complexes suspended in hexane. The suspension turned into a clear solution within several minutes to hours. After additional stirring for 2 h, the reaction mixture was filtrated through a Celite pad and the solvent removed in vacuo. After drying for several hours, the solid was dissolved in hexane and crystallized at −45 °C. The heteroleptic aluminate complexes were obtained with one molecule of hexane in the crystal lattice within 16 h to several weeks in moderate yields.

Procedure C. In a glovebox, $Ln(AlMe_4)_3$ was dissolved in hexane, and a toluene solution of $[Me_2Al(\mu\text{-}O_2CAr^R)]_2$ (2 or 3 equiv) was slowly added. After stirring overnight at ambient temperature the solvent was removed in vacuo. The product was isolated via extraction into toluene, washed several times with hexane, and dried until constant weight under reduced pressure.

Procedure D. In a glovebox, $Ln(AlMe_4)_3$ was dissolved in hexane, and a toluene suspension of the carboxylic acid, HO_2CAr^R (1−4 equiv), was slowly added. The solution was stirred at ambient temperature for 18 h. The solvent was removed in vacuo, and the product was isolated via extraction into toluene, washed with hexane, and dried for several hours.

$Y[(O_2CAr^{iPr})_2(\mu\text{-}AlMe_2)]_2[(\mu\text{-}Me)_2AlMe_2]$ (12a). Following procedure A, **2a** (0.623 g, 0.75 mmol) and TMA (0.325 g, 4.50 mmol) yielded **12a** (0.345 g, 36%) as a colorless solid. IR (Nujol): 1604 s, 1593 s, 1573 s, 1513 s, 1429 s, 1377 s, 1364 s, 1298 m, 1190 m, 1161 m, 1111 m, 1072 w, 940 w, 880 m, 768 w, 692 s, 636 w, 623 w, 585 w, 504 w, 481 w, 456 w cm^{-1}. ^1H NMR (C_6D_6): δ 7.03 (s, 8 H, Ar-*H*), 3.20 (septet, $^3J_{HH}$ = 6.7 Hz, 8 H, o-C*H*Me_2), 2.73 (septet, $^3J_{HH}$ = 7.0 Hz, 4 H, p-C*H*Me_2), 1.22 (d, $^3J_{HH}$ = 6.7 Hz, 48 H, o-CH*Me*$_2$), 1.19 (d, $^3J_{HH}$ = 7.0 Hz, 24 H, p-CH*Me*$_2$), −0.08 (s, 12 H, Al*Me*$_2$), −0.41 (s, 12 H, Al*Me*$_4$). $^{13}C\{^1H\}$ NMR (C_6D_6): δ 181.7 (*C*OO), 151.0, 144.7, 132.0, 121.3, 34.8 (p-*C*HMe_2), 32.1 (o-*C*HMe_2), 24.6 (o-CH*Me*$_2$), 24.1 (p-CH*Me*$_2$), 0.0, −10.4. Anal. Calcd for $C_{72}H_{116}Al_3O_8Y$: C, 67.58; H, 9.14. Found: C, 66.02; H, 9.28.

$La[(O_2CAr^{iPr})_2(\mu\text{-}AlMe_2)]_2[(\mu\text{-}Me)_2AlMe_2]$(hexane) (12b). Following procedure B, **2b** (0.440 g, 0.50 mmol) and TMA (0.126 g, 1.75 mmol) gave **12b** (0.321 g, 45%) as a colorless solid. IR (Nujol): 1618 m, 1527 s, 1425 s, 1365 s, 1350 m, 1331 m, 1316 m, 1196 w, 1150 w, 1108 w, 1086 w, 940 w, 877 m, 779 w, 698 s, 632 w, 592 w, 489 w, 459 w, 406 w cm^{-1}. ^1H NMR (C_6D_6): δ 7.06 (s, 8 H, Ar-*H*), 3.27 (septet, $^3J_{HH}$ = 7.0 Hz, 8 H, o-C*H*Me_2), 2.72 (sp, $^3J_{HH}$ = 6.6 Hz, 4 H, p-C*H*Me_2), 1.28 (d, $^3J_{HH}$ = 7.0 Hz, 48 H, o-CH*Me*$_2$), 1.17 (d, $^3J_{HH}$ = 6.6 Hz, 24 H, p-CH*Me*$_2$), 0.13 (s, 12 H, Al*Me*$_2$), −0.62 (s, 12 H, Al*Me*$_4$). $^{13}C\{^1H\}$ NMR (C_6D_6): δ 183.3 (*C*OO), 151.4, 144.8, 131.8, 121.3, 34.8 (p-*C*HMe_2), 32.2 (o-*C*HMe_2) 24.6 (o-CH*Me*$_2$), 24.0 (p-CH*Me*$_2$), 3.9 (Al*Me*$_2$), −10.8 (Al*Me*$_4$). Anal. Calcd for $C_{78}H_{130}Al_3LaO_8$: C, 66.17; H, 9.26. Found: C, 66.14; H, 9.45.

$Nd[(O_2CAr^{iPr})_2(\mu\text{-}AlMe_2)]_2[(\mu\text{-}Me)_2AlMe_2]$(hexane) (12c). Following procedure B, **2c** (0.445 g, 0.50 mmol) and TMA (0.126 g, 1.75 mmol) yielded **12c** (0.285 g, 40%) as light blue crystals. IR (Nujol): 1618 m, 1526 s, 1429 s, 1363 s, 1351 m, 1331 m, 1317 m, 1195 w, 1157 w, 1109 w, 1086 w, 941 w, 887 w, 876 w, 777 w, 698 s, 633 w, 587 w, 486 w, 460 w, 408 w. Anal. Calcd for $C_{78}H_{130}Al_3NdO_8$: C, 65.93; H, 9.22. Found: C, 66.12; H, 9.36.

$Gd[(O_2CAr^{iPr})_2(\mu\text{-}AlMe_2)]_2[(\mu\text{-}Me)_2AlMe_2]$(hexane) (12d). Following procedure B, **2d** (0.451 g, 0.50 mmol) and TMA (0.126 g, 1.75 mmol) yielded **12d** (0.293 g, 41%) as a colorless solid. IR (Nujol): 1624 s, 1606 m, 1574 w, 1427 s, 1364 s, 1350 s, 1330 m, 1316 s, 1196 m, 1154 m, 1108 m, 1086 w, 940 w, 888 m, 877 m, 778 m, 698 vs, 631 w, 587 m, 490 w, 468 w. Anal. Calcd for $C_{78}H_{130}Al_3GdO_8$: C, 65.28; H, 9.14. Found: C, 65.14; H, 8.75.

$Lu[(O_2CAr^{iPr})_2(\mu\text{-}AlMe_2)]_2[(\mu\text{-}Me)_2AlMe_2]$ (12e). Following procedure A, **2e** (0.459 g, 0.50 mmol) and TMA (0.216 g, 3.00 mmol) gave **12e** (0.250 g, 37%) as a colorless solid. IR (Nujol): 1596 m, 1573 m, 1542 m, 1513 m, 1423 s, 1364 s, 1317 w, 1302 w, 1190 w, 1160 w, 1110 w, 1072 w, 940 w, 878 m, 767 w, 693 s, 632 w, 617 w, 584 w, 476 w, 456 w, 414 w cm^{-1}. ^1H NMR (C_6D_6): δ 6.98 (s, 8 H, Ar-*H*), 3.11 (septet, $^3J_{HH}$ = 6.6 Hz, 8 H, o-C*H*Me_2), 2.73 (septet, $^3J_{HH}$ = 6.6 Hz, 4 H, p-C*H*Me_2), 1.20 (d, $^3J_{HH}$ = 6.6 Hz, 72 H, o/p-CH*Me*$_2$), 0.10 (s, 12 H, Al*Me*$_2$), −0.33 (s, 12 H, Al*Me*$_4$). $^{13}C\{^1H\}$ NMR (C_6D_6): δ 181.1 (*C*OO), 150.6, 144.4, 132.5, 121.2, 34.8 (p-*C*HMe_2), 32.1 (o-*C*HMe_2), 24.7 (o-CH*Me*$_2$), 24.1 (p-CH*Me*$_2$), 0.3, −10.3. Anal. Calcd for $C_{72}H_{116}Al_3LuO_8$: C, 63.33; H, 8.56. Found: C, 62.98; H, 8.49.

$La[(O_2CAr^{iPr})_2(\mu\text{-}AlEt_2)]_2[(\mu\text{-}Et)_2AlEt_2]$(hexane) (13a). Following procedure B, **2b** (0.440 g, 0.50 mmol) and TEA (1.75 mL of a 1.0 M hexane solution, 1.75 mmol) yielded **13a** (0.262 g, 34%) as colorless crystals. IR (Nujol): 1620 s, 1606 m, 1573 w, 1526 s, 1421 s, 1364 m, 1350 m, 1329 m, 1314 m, 1156 w, 1109 w, 1086 w, 988 w, 953 w, 877 m, 766 w, 657 s, 640 m, 604 w cm^{-1}. ^1H NMR (C_6D_6): δ 7.05 (s, 8 H, Ar-*H*), 3.20 (septet, $^3J_{HH}$ = 6.6 Hz, 8 H, o-C*H*Me_2), 2.73 (septet, $^3J_{HH}$ = 7.0 Hz, 4 H, p-C*H*Me_2), 1.67 (t, $^3J_{HH}$ = 7.7 Hz, 12 H, AlEt), 1.30 (d, $^3J_{HH}$ = 6.6 Hz, 48 H, o-CH*Me*$_2$), 1.17 (d, $^3J_{HH}$ = 7.0 Hz, 24 H, p-CH*Me*$_2$), 1.13 (t, $^3J_{HH}$ = 8.1 Hz, 12 H, AlEt), 0.59 (q, $^3J_{HH}$ = 7.7 Hz, 8 H, AlEt), 0.15 (q, $^3J_{HH}$ = 8.1 Hz, 8 H, AlEt). $^{13}C\{^1H\}$ NMR (C_6D_6): δ 182.6 (*C*OO), 151.2, 144.9, 131.8, 121.4, 34.8 (p-*C*HMe_2), 32.2 (o-*C*HMe_2) 24.7 (o-CH*Me*$_2$), 24.0 (p-CH*Me*$_2$), 14.9 (br, AlEt), 13.1 (AlEt), 8.9 (AlEt), −0.2 (br, AlEt). Anal. Calcd for $C_{86}H_{146}Al_3LaO_8$: C, 67.60; H, 9.63. Found: C, 67.72; H, 9.82.

$Nd[(O_2CAr^{iPr})_2(\mu\text{-}AlEt_2)]_2[(\mu\text{-}Et)_2AlEt_2]$(hexane) (13b). Following procedure B, **2c** (0.445 g, 0.50 mmol) and TEA (1.75 mL of a 1.0 M hexane solution, 1.75 mmol) yielded **13c** (0.132 g, 17%) as light blue crystals. IR (Nujol): 1620 m, 1573 w, 1524 s, 1424 m, 1348 m, 1328 m, 1314 m, 1155 w, 1109 w, 1086 w, 985 w, 954 w, 878 m, 788 w, 658 s, 634 m, 598 w cm^{-1}. Anal. Calcd for $C_{86}H_{146}Al_3NdO_8$: C, 67.37; H, 9.60. Found: C, 66.13; H, 9.30.

$Y[(O_2CAr^{Me})_2(\mu\text{-}AlMe_2)]_3$ (14a). Following procedure C, $Y(AlMe_4)_3$ (0.350 g, 1.00 mmol) and $[Me_2Al(\mu\text{-}O_2CAr^{Me})]_2$ (0.661 g, 1.50 mmol) yielded **14a** (∼80%) together with a mixture of different alkylated byproducts, which could not be separated. ^1H NMR (C_6D_6): δ 6.58 (s, 12 H, Ar-*H*), 2.41 (s, 36 H, o-*Me*), 1.99 (s, 18 H, p-*Me*), −0.54 (s, 18 H, Al*Me*$_2$). $^{13}C\{^1H\}$ NMR (C_6D_6): δ 181.6 (*C*OO), 139.4, 134.9, 133.0, 128.6, 21.1 (p-*Me*), 20.4 (o-*Me*), −9.9 (Al*Me*$_2$).

La[(O_2CAr^{Me})$_2$(μ-$AlMe_2$)]$_3$ (14b). Following procedure C, La($AlMe_4$)$_3$ (0.400 g, 1.00 mmol) and [Me_2Al(μ-O_2CAr^{Me})]$_2$ (0.661 g, 1.50 mmol) gave **14b** (~70%) together with other alkylated byproducts, which could not be separated. ^{1}H NMR (C_6D_6): δ 6.57 (s, 12 H, Ar-*H*), 2.43 (s, 36 H, o-*Me*), 1.99 (s, 18 H, p-*Me*), −0.54 (s, 18 H, AlMe_2).

{**Y(O_2CAr^{tBu})[(μ-Me)$_2$$AlMe_2$]$_2$}$_2$ (15a).** Following procedure D, Y($AlMe_4$)$_3$ (0.175 g, 0.50 mmol) and HO_2CAr^{tBu} (0.145 g, 0.50 mmol) yielded **15a** (0.253 g, 87%) as a colorless solid. IR (Nujol): 1598 w, 1531 s, 1266 w, 1244 w, 1215 m, 1192 m, 1088 w, 880 w, 797 w, 779 w, 761 w, 721 m, 698 m, 692 s, 662 w, 580 m, 544 m cm^{-1}. ^{1}H NMR (C_6D_6): δ 7.50 (s, 2 H, Ar-*H*), 1.47 (s, 18 H, o-CMe_3), 1.31 (s, 9 H, p-CMe_3), −0.12 (s, br, 24 H, AlMe_4). ^{13}C{^{1}H} NMR (C_6D_6): δ 184.9 (*C*OO), 150.8, 145.3, 125.2, 123.8, 37.8 (o-*C*Me_3), 35.0 (p-*C*Me_3), 33.3 (o-CMe_3), 31.2 (p-CMe_3), 2.2 (br, AlMe_4). Anal. Calcd for $C_{54}H_{106}Al_4O_4Y_2$: C, 58.69; H, 9.67. Found: C, 58.86; H, 9.72.

{**La(O_2CAr^{tBu})[(μ-Me)$_2$$AlMe_2$]$_2$}$_2$ (15b).** Following procedure D, La($AlMe_4$)$_3$ (0.200 g, 0.50 mmol) and HO_2CAr^{tBu} (0.145 g, 0.50 mmol) yielded **15b** (0.281 g, 93%) as a colorless solid. IR (Nujol): 1598 w, 1525 s, 1265 w, 1242 w, 1204 m, 1186 m, 1088 w, 879 w, 799 w, 778 w, 761 w, 719 m, 692 s, 583 m, 573 m, 551 w cm^{-1}. ^{1}H NMR (C_6D_6): δ 7.50 (s, 2 H, Ar-*H*), 1.50 (s, 18 H, o-CMe_3), 1.26 (s, 9 H, p-CMe_3), −0.03 (s, br, 24 H, AlMe_4). ^{13}C{^{1}H} NMR (C_6D_6): δ 185.6 (*C*OO), 151.1, 145.1, 123.3, 122.9, 37.7 (o-*C*Me_3), 35.0 (p-*C*Me_3), 33.4 (o-CMe_3), 31.2 (p-CMe_3), 7.1 (AlMe_4). Anal. Calcd for $C_{54}H_{106}Al_4La_2O_4$: C, 53.82; H, 8.87. Found: C, 53.70; H, 8.91.

{**Nd(O_2CAr^{tBu})[(μ-Me)$_2$$AlMe_2$]$_2$}$_2$ (15c).** Following procedure D, Nd($AlMe_4$)$_3$ (0.203 g, 0.50 mmol) and HO_2CAr^{tBu} (0.145 g, 0.50 mmol) gave **15c** (0.287 g, 94%) as a bluish solid. IR (Nujol): 1598 w, 1524 s, 1554 s, 1362 s, 1266 w, 1242 w, 1206 m, 1187 m, 1088 w, 879 w, 798 w, 778 w, 761 w, 719 s, 691 s, 573 m, 548 w cm^{-1}. ^{1}H NMR (C_6D_6): δ 9.66 (s, br, 48 H, AlMe_4), 8.26 (s, 4 H, Ar-*H*), 2.04 (s, 18 H, p-CMe_3), −1.66 (s, 36 H, o-CMe_3). Anal. Calcd for $C_{54}H_{106}Al_4Nd_2O_4$: C, 53.34; H, 8.79. Found: C, 53.25; H, 8.83.

{**Y(O_2CAr^{Ph})[(μ-Me)$_2$$AlMe_2$]$_2$}$_2$ (16a).** Following procedure D, Y($AlMe_4$)$_3$ (0.140 g, 0.40 mmol) and HO_2CAr^{Ph} (0.110 g, 0.40 mmol) yielded **16a** (0.138 g, 64%) as a colorless solid. IR (Nujol): 1944 w, 1876 w, 1684 w, 1584 m, 1561 s, 1496 m, 1402 m, 1303 w, 1214 w, 1195 w, 1158 w, 1072 w, 1029 w, 918 w, 816 w, 780 w, 758 m, 722 m, 698 s, 647 w, 615 w, 595 w, 575 m, 521 w, 483 w cm^{-1}. ^{1}H NMR (C_6D_6): δ 7.32 (d, $^3J_{HH}$ = 7.6 Hz, 8 H, Ph-H_{ortho}), 7.21 (t, $^3J_{HH}$ = 7.6, 8 H, Ph-H_{meta}), 7.10 (t, $^3J_{HH}$ = 7.6 Hz, 4 H, Ph-H_{para}), 6.92 (s, 6 H, Ar-*H*), −0.43 (s, br, 48 H, AlMe_4). ^{1}H NMR (toluene-d_8, −80 °C): δ 7.3−7.0 (m, 20 H, Ph-*H*), 6.80 (s, 6 H, Ar-*H*), 0.14 (s, br, 12 H, Y-*Me*-Al), −0.27 (s, 12 H, AlMe_2), −0.53 (s, br, 12 H, Y-*Me*-Al), −0.72 (s, 12 H, AlMe_2). ^{13}C{^{1}H} NMR (C_6D_6): δ 177.8 (d, $^2J_{CY}$ = 3.1 Hz, *C*OO), 141.6, 141.4, 132.4, 130.5, 130.2, 129.2, 128.9, 128.7, 1.5 (br, AlMe_4). Anal. Calcd for $C_{54}H_{74}Al_4O_4Y_2$: C, 60.45; H, 6.95. Found: C, 59.86; H, 6.72.

{**La(O_2CAr^{Ph})[(μ-Me)$_2$$AlMe_2$]$_2$}$_2$ (16b).** Following procedure D, La($AlMe_4$)$_3$ (0.184 g, 0.46 mmol) and HO_2CAr^{Ph} (0.126 g, 0.46 mmol) yielded **16b** (0.160 g, 59%) as a colorless solid. IR (Nujol): 1967 w, 1948 w, 1892 w, 1810 w, 1586 m, 1574 m, 1543 s, 1513 m, 1495 m, 1311 w, 1210 m, 1186 s, 1151 m, 1072 w, 1028 w, 914 w, 816 w, 784 w, 758 s, 717 s, 698 s, 648 w, 602 w, 573 m, 544 m, 528 m, 484 w cm^{-1}. ^{1}H NMR (C_6D_6): δ 7.33 (d, $^3J_{HH}$ = 7.3 Hz, 8 H, Ph-H_{ortho}), 7.18 (t, $^3J_{HH}$ = 7.3, 8 H, Ph-H_{meta}), 7.05 (t, $^3J_{HH}$ = 7.3 Hz, 4 H, Ph-H_{para}), 6.90 (s, 6 H, Ar-*H*), −0.33 (s, 48 H, AlMe_4). ^{13}C{^{1}H} NMR (C_6D_6): δ 180.5 (*C*OO), 140.4, 140.3, 132.2, 130.3, 129.7, 129.3, 129.0, 128.3, 4.3 (br, AlMe_4). Anal. Calcd for $C_{54}H_{74}Al_4La_2O_4$: C, 55.30; H, 6.36. Found: C, 55.41; H, 6.43.

General Procedure for the Synthesis of Alkylaluminum Carboxylates. In a glovebox, 1 equiv of TMA or TEA was slowly added to a cooled hexane suspension (−35 °C) of the aromatic carboxylic acid. The solution became clear immediately except for **9**, and gas evolution (CH_4, C_2H_6) was observed. After stirring at ambient temperature for an additional 3 h the solvent was removed in vacuo, yielding the products as white solids in quantitative yields.

[Me_2Al(μ-$O_2CC_6H_2Me_3$-2,4,6)]$_2$ (6). Following the procedure described above, HO_2CAr^{Me} (0.328 g, 2.00 mmol) and TMA (0.144 g, 2.00 mmol) yielded **6** (0.439 g, >99%) as a colorless solid. IR (Nujol): 1722 w, 1613 m, 1524 s, 1502 s, 1195 m, 1034 w, 872 w, 847 m, 788 w, 701 s, 665 m, 636 m, 582 m, 517 m cm^{-1}. ^{1}H NMR (C_6D_6): δ 6.52 (s, 4 H, Ar-*H*), 2.34 (s, 12 H, o-*Me*), 1.95 (s, 6 H, p-*Me*), −0.25 (s, 12 H, AlMe_2). ^{13}C{^{1}H} NMR (C_6D_6): δ 177.9 (*C*OO), 141.3, 137.4, 130.3, 129.8, 21.0 (o-*Me*), 20.9 (p-*Me*), −10.6 (AlMe_2). Anal. Calcd for $C_{24}H_{34}Al_2O_4$: C, 65.44; H, 7.78. Found: C, 65.50; H, 7.75.

[Me_2Al(μ-$O_2CC_6H_2iPr_3$-2,4,6)]$_2$ (7). Following the procedure described above, HO_2CAr^{iPr} (0.497 g, 2.00 mmol) and TMA (0.144 g, 2.00 mmol) gave **7** (0.605 g, >99%) as a colorless solid. IR (Nujol): 1771 w, 1591 s, 1483 m, sh, 1363 s, 1319 w, 1296 w, 1194 m, 1162 w, 1112 w, 1103 w, 1070 w, 941 w, 880 w, 772 w, 698 s, br, 630 w, 574 w, 496 w, 465 w cm^{-1}. ^{1}H NMR (C_6D_6): δ 7.05 (s, 4 H, Ar-*H*), 3.20 (septet, $^3J_{HH}$ = 6.6 Hz, 4 H, o-C*H*Me_2), 2.70 (septet, $^3J_{HH}$ = 7.0 Hz, 2 H, p-C*H*Me_2), 1.27 (d, $^3J_{HH}$ = 6.6 Hz, 24 H, o-CHMe_2), 1.15 (d, $^3J_{HH}$ = 7.0 Hz, 12 H, p-CHMe_2), −0.23 (s, 12 H, AlMe_2). ^{13}C{^{1}H} NMR (C_6D_6): δ 179.8 (*C*OO), 151.3, 144.8, 131.7, 121.6, 34.8 (p-*C*HMe_2), 32.3 (o-*C*HMe_2), 24.3 (o-CHMe_2), 24.0 (p-CHMe_2), −10.9 (AlMe_2). Anal. Calcd for $C_{36}H_{58}Al_2O_4$: C, 71.02; H, 9.60. Found: C, 70.81; H, 9.45.

[Me_2Al(μ-$O_2CC_6H_2tBu_3$-2,4,6)]$_2$ (8). Following the procedure described above, HO_2CAr^{tBu} (0.363 g, 1.25 mmol) and TMA (0.090 g, 1.25 mmol) yielded **8** (0.340 g, 98%) as a colorless solid. IR (Nujol): 1593 s, 1416 m, 1364 m, 1266 w, 1243 w, 1196 m, 1104 w, 940 w, 879 w, 786 w, 697 s, 623 w, 585 w, 574 w, 492 w, 447 w cm^{-1}. ^{1}H NMR (C_6D_6): δ 7.54 (s, 4 H, Ar-*H*), 1.53 (s, 36 H, o-CMe_3), 1.25 (s, 18 H, p-CMe_3), −0.27 (s, 12 H, AlMe_2). ^{13}C{^{1}H} NMR (C_6D_6): δ 181.0 (*C*OO), 151.1, 146.7, 129.8, 122.8, 37.5 (p-*C*Me_3), 35.1 (o-*C*Me_3), 33.0 (o-CMe_3), 31.3 (p-CMe_3), −9.6 (AlMe_2). Anal. Calcd for $C_{42}H_{70}Al_2O_4$: C, 72.80; H, 10.18. Found: C, 72.93; H, 10.09.

[Me_2Al(μ-$O_2CC_6H_3Ph_2$-2,6)]$_2$ (9). Following the procedure described above, HO_2CAr^{Ph} (0.262 g, 1.00 mmol) and TMA (0.072 g, 1.00 mmol) yielded **9** (0.330 g, >99%) as a colorless solid. IR (Nujol): 1619 vs, 1599 s, 1578 s, 1495 s, 1408 s, 1302 w, 1190 m, 1168 w, 1072 m, 1029 w, 917 w, 817 w, 783 m, 758 s, 736 m, 696 vs, br, 644 m, 575 m, 524 m, 484 m, 475 m cm^{-1}. ^{1}H NMR (C_6D_6): δ 7.30−7.16 (m, 10 H, Ar-*H*, *Ph*), 7.04−6.96 (m, 3 H, Ar-*H*, *Ph*), −1.05 (s, 12 H, AlMe_2). ^{13}C{^{1}H} NMR (C_6D_6): δ 175.1 (*C*OO), 141.4, 140.7, 133.4, 130.0, 129.7, 129.0, 128.9, 128.7, −9.6 (AlMe_2). Anal. Calcd for $C_{42}H_{38}Al_2O_4$: C, 76.35; H, 5.80. Found: C, 75.96; H, 5.95.

[Me_2Al(μ-$O_2CC_6H_3Mes_2$-2,6)]$_2$ (10). Following the procedure described above, HO_2CAr^{Mes} (0.346 g, 1.00 mmol) and TMA (0.072 g, 1.00 mmol) gave **10** (0.410 g, >99%) as a colorless solid. IR (Nujol): 1612 s, 1584 m, 1546 w, 1402 m, 1308 w, 1192 m, 1169 w, 1066 w, 1032 w, 1014 w, 848 m, 820 w, 784 m, 735 m, 692 s, 585 m, 570 w, 498 w cm^{-1}. ^{1}H NMR (C_6D_6): δ 7.02 (t, $^3J_{HH}$ = 7.7 Hz, 2 H, p-Ar-*H*), 6.90 (s, 8 H, m-Mes-*H*), 6.76 (d, $^3J_{HH}$ = 7.7 Hz, 4 H, m-Ar-*H*), 2.23 (s, 12 H, p-Mes-*Me*), 2.02 (s, 24 H, o-Mes-*Me*), −1.03 (s, 12 H, AlMe_2). ^{13}C{^{1}H} NMR (C_6D_6): δ 174.5 (*C*OO), 140.7, 137.1, 137.0, 135.6, 133.8, 131.1, 129.3, 128.8, 21.1 (p-*Me*), 20.6 (o-*Me*), −11.6 (AlMe_2). Anal. Calcd for $C_{54}H_{62}Al_2O_4$: C, 78.23; H, 7.54. Found: C, 78.09; H, 7.43.

[Et_2Al(μ-$O_2CC_6H_2iPr_3$-2,4,6)]$_2$ (11). Following the procedure described above, HO_2CAr^{iPr} (0.497 g, 2.00 mmol) and TEA (0.228 g, 2.00 mmol) yielded **11** (0.663 g, >99%) as a colorless solid. IR (Nujol): 1592 vs, 1487 s, 1443 vs, 1364 s, 1320 w, 1195 w, 1163 w, 1111 w, 1071 w, 988 w, 951 w, 920 w, 877 w, 772 w, 721 w,

Table 6. Crystallographic Data for Compounds 1b′, 1c′, 7, 15b, and 15c

	1b′	1c′	7	15b	15c
formula	$C_{68}H_{90}La_2O_{16}S_4$	$C_{36}H_{51}NdO_9S_3$	$C_{36}H_{58}Al_2O_4$	$C_{54}H_{106}Al_4La_2O_4$	$C_{54}H_{106}Al_4Nd_2O_4$
fw	1569.50	868.22	608.78	1205.13	1215.79
color/habit	colorless/fragment	pale blue/fragment	colorless/fragment	colorless/fragment	pale blue/fragment
cryst dimens (mm^3)	0.16 × 0.42 × 0.53	0.50 × 0.64 × 0.64	0.28 × 0.36 × 0.45	0.23 × 0.30 × 0.33	0.18 × 0.18 × 0.51
cryst syst	monoclinic	triclinic	monoclinic	monoclinic	monoclinic
space group	*C*2/*c* (no. 15)	$P\bar{1}$ (no. 2)	$P2_1/n$ (no. 14)	*C*2/*c* (no. 15)	*C*2/*c* (no. 15)
a, Å	26.0737(3)	9.6455(1)	10.0759(1)	23.7992(2)	23.5611(2)
b, Å	18.9165(2)	15.2867(2)	10.0962(1)	19.6717(1)	19.4031(1)
c, Å	16.9219(2)	15.6504(2)	19.2370(2)	15.1649(1)	15.2363(1)
α, deg	90	116.9415(5)	90	90	90
β, deg	120.9598(6)	99.3467(7)	104.2331(3)	114.6295(3)	113.5901(3)
γ, deg	90	94.9344(7)	90	90	90
V, $Å^3$	7157.16(15)	1996.17(4)	1896.88(3)	6453.84(8)	6383.32(8)
Z	4	2	2	4	4
T, K	123	123	153	173	123
D_{calcd}, g cm^{-3}	1.457	1.444	1.066	1.240	1.265
μ, mm^{-1}	1.357	1.506	0.109	1.397	1.700
F(000)	3216	894	664	2512	2536
θ range, deg	2.15−25.34	1.50−25.35	2.58−25.33	1.73−25.33	1.41−25.33
index ranges (*h*, *k*, *l*)	±31, ±22, ±20	±11, ±18, ±18	±12, ±12, ±23	±28, ±23, ±18	±28, ±23, ±18
no. of rflns collected	18 159	39 487	41 190	72 245	75 409
no. of indep rflns/R_{int}	6433/0.024	7305/0.038	3455/0.040	5898/0.046	5856/0.041
no. of obsd rflns ($I > 2\sigma(I)$)	5786	7191	3143	4835	5152
no. of data/restraints/params	6433/0/581	7305/0/641	3455/0/318	5898/0/394	5856/0 /502
R1/wR2 ($I > 2\sigma(I)$)[a]	0.0221/0.0498	0.0196/0.0502	0.0348/0.0913	0.0244/0.0564	0.0179/0.0397
R1/wR2 (all data)[a]	0.0269/0.0520	0.0201/0.0504	0.0388/0.0945	0.0348/0.0602	0.0230/0.0415
GOF (on F^2)[a]	1.023	1.080	1.028	1.039	1.023
largest diff peak and hole (e $Å^{-3}$)	+0.62/−0.44	+1.44/−0.81	+0.33/−0.21	+0.70/−0.87	+0.69/−0.33

[a] $R1 = \sum(||F_o| - |F_c||)/\sum|F_o|$; $wR2 = \{\sum[w(F_o^2 - F_c^2)^2]/\sum[w(F_o^2)^2]\}^{1/2}$; $GOF = \{\sum[w(F_o^2 - F_c^2)^2]/(n - p)\}^{1/2}$

661 m, 634 m, 540 w, 506 w, 494 w, 465 w cm^{-1}. ^1H NMR (C_6D_6): δ 7.07 (s, 4 H, Ar-*H*), 3.23 (septet, $^3J_{HH} = 6.8$ Hz, 4 H, o-C*H*Me_2), 2.70 (septet, $^3J_{HH} = 6.8$ Hz, 2 H, p-C*H*Me_2), 1.33 (d, $^3J_{HH} = 6.8$ Hz, 24 H, o-CH*Me*$_2$), 1.32 (t, $^3J_{HH} = 8.0$ Hz, 12 H, $AlCH_2CH_3$), 1.14 (d, $^3J_{HH} = 6.8$ Hz, 12 H, p-CH*Me*$_2$), 0.38 (q, $^3J_{HH} = 8.0$ Hz, 8 H, $AlCH_2CH_3$). $^{13}C\{^1H\}$ NMR (C_6D_6): δ 180.0 (*C*OO), 151.3, 144.8, 131.5, 121.6, 34.7 (p-*C*HMe_2), 32.4 (o-*C*HMe_2), 24.5 (o-CH*Me*$_2$), 23.9 (p-CH*Me*$_2$), 8.8 ($AlCH_2CH_3$), −1.0 ($AlCH_2CH_3$). Anal. Calcd for $C_{40}H_{66}Al_2O_4$: C, 72.25; H, 10.00. Found: C, 71.81; H, 9.85.

Reaction of 12a with Me_2AlCl. In a glovebox, **12a** (0.448 g, 0.35 mmol) was suspended in 8 mL of hexane, and 1 equiv of Me_2AlCl (0.35 mL of a 1.0 M hexane solution, 0.35 mmol) was added at ambient temperature. Immediately a white precipitate formed. After stirring for an additional 2 h the solid was separated via centrifugation, washed several times with hexane, and dried. Yield: 0.049 g (0.32 mmol, 91%). Anal. Calcd for C_2H_6ClY (**17a**): C, 15.56; H, 3.92. Found: C, 19.11; H, 4.68. The hexane solution was filtrated through a Celite pad, and the solvent was removed in vacuo, yielding 0.431 g of a colorless, crystalline product, which was identified as **7**. Anal. Calcd for $C_{36}H_{58}Al_2O_4$: C, 71.02; H, 9.60. Found: C, 71.51; H, 9.86.

Reaction of 12b with Me_2AlCl. Following the procedure described above, **12b** (0.354 g, 0.25 mmol) and Me_2AlCl (0.25 mL, 0.25 mmol) yielded 0.044 g (0.22 mmol, 86%) of a white solid (**17b**) and 0.314 g of **7**. Anal. Calcd for C_2H_6ClLa (**17b**): C, 11.75; H, 2.96. Found: C, 17.46; H, 4.39. Anal. Calcd for $C_{36}H_{58}Al_2O_4$ (**7**): C, 71.02; H, 9.60. Found: C, 71.33; H, 9.80.

Polymerization of Isoprene. All manipulations were performed in a glovebox under an argon atmosphere. A detailed polymerization procedure for run 8 of Table 5 is described as a typical example. To a solution of **12c** (0.018 g, 0.02 mmol) in 8 mL of hexane was added 2 equiv of Et_2AlCl (5.0 μL, 0.04 mmol), and the mixture was aged at ambient temperature for 30 min before use. After the addition of isoprene (2.0 mL, 20 mmol) the polymerization was carried out at 40 °C for 24 h. The polymerization mixture was poured into a large quantity of acidified 2-propanol containing 0.1% (w/w) 2,6-di-*tert*-butyl-4-methylphenol as a stabilizer. The polymer was washed with 2-propanol and dried under vacuum at ambient temperature to constant weight. The polymer yield was determined gravimetrically.

Polymer Characterization. The molar masses M_w and M_n of the polymers were determined by size exclusion chromatography (SEC). Sample solutions (1.0 mg polymer per mL $CHCl_3$) were filtered through a 0.2 μm syringe filter prior to injection. SEC was operated with a pump supplied by Waters (type: Waters 510), and Ultrastyragel columns with pore sizes of 500, 1000, 10 000, and 100 000 Å were used. The signals were detected by a differential refractometer (Waters 410) and calibrated against polystyrene standards ($M_w/M_n < 1.15$). The flow rate was 1.0 mL min^{-1}. The microstructure of the polyisoprenes was examined via ^{13}C NMR experiments in $CDCl_3$.

Single-Crystal X-ray Structure Determination of Compounds 1b′, 1c′, 7, 13b, 15b, and 15c. General Comments. Crystal data and details of the structure determination are presented in Table 6. Suitable single-crystals for the X-ray diffraction study were grown with standard cooling techniques. Except for **1b′** and **1c′** all preparations were carried out in a glovebox. Crystals were stored under perfluorinated ether, transferred in a Lindemann capillary, fixed, and sealed. Preliminary examination and data collection were carried out on an area detecting system (NONIUS, MACH3, κ-CCD) at the window of a rotating anode (NONIUS, FR591) and graphite-monochromated Mo Kα radiation ($\lambda = 0.71073$ Å). The unit cell parameters were obtained by full-matrix least-squares refinements during the scaling procedure. Data collections were performed at low temperatures (Oxford Cryosystems), each measured with a couple of data sets in rotation scan modus with $\Delta\varphi/\Delta\omega = 1.0$. Intensities were integrated, and the raw data were corrected for Lorentz, polarization, and, arising from the scaling procedure, latent decay and absorption effects. The structures were solved by a combination of direct methods and difference Fourier syntheses. All non-hydrogen atoms were refined with anisotropic displacement parameters. Full-matrix least-squares refinements were carried out by minimizing $\sum w(F_o^2 - F_c^2)^2$ with the SHELXL-97 weighting scheme and stopped at shift/err < 0.004. The final residual electron density maps showed no remarkable features. Neutral atom scattering factors for all atoms and anomalous dispersion corrections for the non-hydrogen atoms were taken from

International Tables for Crystallography. All calculations were performed on an Intel Pentium II PC, with the STRUX-V system, including the programs PLATON, SIR92, and SHELXL-97.[56] *Special*: **1b′**: A disorder over two positions (0.667(4):0.333(4)) of one of the two DMSO ligands could be resolved clearly. Their methyl hydrogen atoms were refined as part of rigid groups, with $d_{C-H} = 0.98$ Å and $U_{iso(H)} = 1.5U_{eq(C)}$. All other hydrogen atoms were located from difference Fourier syntheses and were allowed to refine freely. The X-ray results of a single-crystal grown in a different flask show the same behavior (STOE&Cie. IPDS, $T = 173$ K, $a = 26.050(2)$ Å, $b = 19.021(1)$ Å, $c = 16.954(1)$ Å, $\beta = 120.576(6)°$, $V = 7232.4(9)$ Å^3, disorder 0.671(4):0.329(4)). **1c′**: A disorder over two positions (0.752(3):0.248(3)) of one of the three DMSO ligands could be resolved clearly. The methyl hydrogen atoms were refined as part of rigid groups, with $d_{C-H} = 0.98$ Å and $U_{iso(H)} = 1.5U_{eq(C)}$. All other hydrogen atoms were located from difference Fourier syntheses and were allowed to refine freely. **13b**: $C_{80}H_{132}Al_3LaO_8$, $M_r = 1441.71$, colorless fragment ($0.15 \times 0.20 \times 0.63$ mm^3), monoclinic, *C*2/*c* (No. 15), $a = 25.8264(2)$ Å, $b = 20.4639(2)$ Å, $c = 18.6338(2)$ Å, $\beta = 103.8579(3)°$, $V = 9561.5(2)$ Å^3, $Z = 4$, $d_{calc} = 1.002$ g cm^{-3}, $F_{000} = 3088$, $\mu = 0.517$ mm^{-1}, R1/wR2 ($I > 2\sigma(I)$) = 0.0416/0.1193, R1/wR2 (all data) = 0.0460/0.1224. The result suffers from a severe disordering of the highly mobile isopropyl and ethyl groups, even at low temperatures. Attempts to get better results in the acentric space group *Cc* failed. **15b**: Methyl hydrogen atoms of the tetramethylaluminate ligands were located from difference Fourier syntheses and were allowed to refine freely. All other hydrogen atoms were located from difference Fourier syntheses but either refined as part of rigid rotating groups, with $d_{C-H} = 0.98$ Å and $U_{iso(H)} = 1.5U_{eq(C)}$, or placed in calculated positions and refined using a riding model, with an aromatic d_{C-H} distance of 0.95 Å and $U_{iso(H)} = 1.2U_{eq(C)}$. **15c**: Small extinction effects were corrected with the SHELXL-97 procedure with $\epsilon = 0.00019(2)$. All hydrogen atoms were located from difference Fourier syntheses and were allowed to refine freely. **7**: All hydrogen atoms were located from difference Fourier syntheses and were allowed to refine freely. Crystallographic data (excluding structure factors) for the structures reported in this paper have been deposited with the Cambridge Crystallographic Data Centre as supplementary publication nos. CCDC-289152 (**1b′**), CCDC-298151 (**1c′**), CCDC-298154 (**15b**), CCDC-298155 (**15c**), and CCDC-298153 (**7**). Copies of the data can be obtained free of charge on application to CCDC, 12 Union Road, Cambridge CB2 1EZ, UK (fax: (+44)1223-336-033; e-mail: deposit@ccdc.cam.ac.uk).

(56) (a) *Data Collection Software for Nonius k-CCD Devices*; Delft, The Netherlands, 2001. (b) Otwinowski, Z.; Minor, W. *Methods Enzymol.* **1997**, *276*, 307. (c) Altomare, A.; Cascarano, G.; Giacovazzo, C.; Guagliardi, A.; Burla, M. C.; Polidori, G.; Camalli, M. *J. Appl. Crystallogr.* **1994**, *27*, 435. (d) *International Tables for Crystallography*; Wilson, A. J. C., Ed.; Kluwer Academic Publishers: Dordrecht, The Netherlands, 1992; Vol. C, Tables 6.1.1.4, 4.2.6.8, and 4.2.4.2. (e) Spek, A. L. *PLATON, A Multipurpose Crystallographic Tool*; Utrecht University: Utrecht, The Netherlands, 2001. (f) Sheldrick, G. M. *SHELXL-97*; Universität Göttingen: Göttingen, Germany, 1998.

Acknowledgment. Financial support by the Deutsche Forschungsgemeinschaft and the Fonds der Chemischen Industrie is gratefully acknowledged. F.P. thanks the University of Ljubljana for an "Otto and Karla Likar" student fellowship. We also thank Dr. Lars Friebe for GPC analysis. E.H. thanks Stefanie Neumann for her help during the course of the X-ray measurements of compound **1b′**.

Supporting Information Available: Text giving tables of atomic coordinates, atomic displacement parameters, bond distances and angles, and disorder models for complexes **1b′**, **1c′**, **7**, **13b**, **15b**, and **15c**. This material is available free of charge via the Internet at http://pubs.acs.org.

OM060052I